EUR 4538 e

COMMISSION OF THE EUROPEAN COMMUNITIES

MEASUREMENTS OF NEUTRON ELASTIC SCATTERING FROM CARBON IN THE ENERGY REGION OF 0.50 TO 2.00 MeV

by

N. AHMED, M. COPPOLA and H.-H. KNITTER

1970

Joint Nuclear Research Centre
Geel Establishment - Belgium

Central Bureau for Nuclear Measurements - CBNM

LEGAL NOTICE

This report is on sale at the addresses listed on cover page 4

at the price of FF 5.60	FB 50.—	DM 3.70	Lit. 620	Fl. 4.30

When ordering, please quote the EUR number and the title, which are indicated on the cover of each report.

Printed by Guyot, s.a., Brussels
Luxembourg, November 1970

EUR 4538 e

MEASUREMENTS OF NEUTRON ELASTIC SCATTERING FROM CARBON IN THE ENERGY REGION OF 0.50 to 2.00 MeV
by N. AHMED, M. COPPOLA and H.-H. KNITTER

Commission of the European Communities
Joint Nuclear Research Centre - Geel Establishment (Belgium)
Central Bureau for Nuclear Measurements - CBNM
Luxembourg, November 1970 - 32 Pages - 38 Figures - FB 50.—

Differential cross sections for the elastic scattering of neutrons from carbon have been measured at primary energies between 0.50 and 2.00 MeV in steps of 50 keV. The experimental cross sections were fitted with a five term Legendre polynomial expansion. The obtained B_L-coefficients were then fitted with suited functions of the energy in order to obtain a smooth dependence of the differential cross sections on the primary neutron energy, using a limited number of parameters. A set of recommended differential elastic cross section curves, based on the present measurements, is given.

Integrated elastic cross sections were derived from the fitted B_0-coefficients and are compared with earlier results of other workers.

EUR 4538 e

MEASUREMENTS OF NEUTRON ELASTIC SCATTERING FROM CARBON IN THE ENERGY REGION OF 0.50 to 2.00 MeV
by N. AHMED, M. COPPOLA and H.-H. KNITTER

Commission of the European Communities
Joint Nuclear Research Centre - Geel Establishment (Belgium)
Central Bureau for Nuclear Measurements - CBNM
Luxembourg, November 1970 - 32 Pages - 38 Figures - FB 50.—

Differential cross sections for the elastic scattering of neutrons from carbon have been measured at primary energies between 0.50 and 2.00 MeV in steps of 50 keV. The experimental cross sections were fitted with a five term Legendre polynomial expansion. The obtained B_L-coefficients were then fitted with suited functions of the energy in order to obtain a smooth dependence of the differential cross sections on the primary neutron energy, using a limited number of parameters. A set of recommended differential elastic cross section curves, based on the present measurements, is given.

Integrated elastic cross sections were derived from the fitted B_0-coefficients and are compared with earlier results of other workers.

EUR 4538 e

MEASUREMENTS OF NEUTRON ELASTIC SCATTERING FROM CARBON IN THE ENERGY REGION OF 0.50 to 2.00 MeV
by N. AHMED, M. COPPOLA and H.-H. KNITTER

Commission of the European Communities
Joint Nuclear Research Centre - Geel Establishment (Belgium)
Central Bureau for Nuclear Measurements - CBNM
Luxembourg, November 1970 - 32 Pages - 38 Figures - FB 50.—

Differential cross sections for the elastic scattering of neutrons from carbon have been measured at primary energies between 0.50 and 2.00 MeV in steps of 50 keV. The experimental cross sections were fitted with a five term Legendre polynomial expansion. The obtained B_L-coefficients were then fitted with suited functions of the energy in order to obtain a smooth dependence of the differential cross sections on the primary neutron energy, using a limited number of parameters. A set of recommended differential elastic cross section curves, based on the present measurements, is given.

Integrated elastic cross sections were derived from the fitted B_0-coefficients and are compared with earlier results of other workers.

EUR 4538 e

COMMISSION OF THE EUROPEAN COMMUNITIES

MEASUREMENTS OF NEUTRON ELASTIC SCATTERING FROM CARBON IN THE ENERGY REGION OF 0.50 TO 2.00 MeV

by

N. AHMED, M. COPPOLA and H.-H. KNITTER

1970

Joint Nuclear Research Centre
Geel Establishment - Belgium

Central Bureau for Nuclear Measurements - CBNM

ABSTRACT

Differential cross sections for the elastic scattering of neutrons from carbon have been measured at primary energies between 0.50 and 2.00 MeV in steps of 50 keV. The experimental cross sections were fitted with a five term Legendre polynomial expansion. The obtained B_L-coefficients were then fitted with suited functions of the energy in order to obtain a smooth dependence of the differential cross sections on the primary neutron energy, using a limited number of parameters. A set of recommended differential elastic cross section curves, based on the present measurements, is given.

Integrated elastic cross sections were derived from the fitted B_0-coefficients and are compared with earlier results of other workers.

KEYWORDS

MEASUREMENTS
NEUTRONS
ELASTIC SCATTERING
CARBON
CROSS SECTIONS
ENERGY
LEGENDRE FUNCTIONS
EXPANSION
MATHEMATICS

1. INTRODUCTION [x)]

The accurate knowledge of the neutron cross sections of carbon is of actual importance and usefulness in the field of neutron scattering measurements. The ^{12}C nucleus has its first excited state at 4.4 MeV and the nuclear reactions that can be induced by neutrons with lower energies are elastic scattering and neutron capture. The (n, γ) cross section is 1.86 mb in the neighbourhood of 0.1 eV [1] and becomes negligible as the incoming neutron energy increases. So the contribution from (n, γ) cross sections is not to be taken into account in the present investigation. The total neutron cross section of carbon shows no resonance structure below 2 MeV and can be represented by simple parametric expansions. For these reasons the neutron cross section of carbon below 2.00 MeV is well suited to be used as a standard for the determination of the neutron scattering cross sections of other elements.

In addition, carbon samples are very easy to be prepared and analysed. Their use as standard samples is especially indicated in neutron scattering experiments, when the $^{7}Li(p, n)^{7}Be$ neutron producing reaction is used above 0.5 MeV. In fact, the other most commonly used standard material, that is polyethylene, can hardly be utilised when more than one primary neutron group is present. In the past, neutron elastic scattering cross sections of carbon up to 4.1 MeV have been measured by several authors [2-7], using methods other than time-of-flight.

In the recent years, the use of the time-of-flight technique has considerably contributed in improving the knowledge of neutron elastic and inelastic scattering processes. Such a technique substantially increases the experimental response rate resulting in a significant improvement of the energy resolution and of the precision of the measurements.

In the present investigations the time-of-flight technique has been used and an extensive study of the neutron elastic scattering measurements on carbon has been performed in the neutron energy region from 0.50 to 2.00 MeV.

2. EXPERIMENTAL EQUIPMENT AND PROCEDURE

The measurements were carried out at the 3 MV Van de Graaff accelerator of CBNM using fast neutron time-of-flight technique. A pulsed ion beam of 1 ns pulse width and 1 MHz repetition rate was focussed on the neutron producing target. The layout of the experimental set up is shown in Fig. 1.

For the production of neutrons two different reactions were used. Between 0.50 and 0.70 MeV neutrons were produced through the $^{7}Li(p, n)^{7}Be$ reaction using a solid LiF target. Above 0.75 MeV neutrons were obtained by the $T(p, n)^{3}He$ reaction with occluded Ti-T targets. The target thicknesses and the scattering geometry were chosen in such a way that the total neutron energy spreads

x) Manuscript received on 2 June 1970

were between 30 and 45 keV for all the measurements. The neutrons emitted from the target around zero degree with respect to the direction of the incoming ion-bursts were scattered from the sample and collimated towards three detectors kept in large shieldings at an equal distance of 141.0 cm from the scatterer. The sample was positioned 15.0 cm away from the target.
The detectors consisted of cylindrical NE 102A plastic scintillators, 5.0 cm x 2.5 cm mounted on AVP 56/03 photomultipliers. The fast outputs of the detectors provided the start signals for the time-to-pulse height converters. The stop signals were taken from a pick-up loop placed before the target at a distance of about 30 cm. The output pulses of the converters were registered in three different memory sections of a 4096 channel pulse height analyser. The overall time resolution of such a neutron time-of-flight spectrometer, including the ion pulse width of the accelerator, was around 2.3 nsec.
The relative neutron fluence was measured by means of an additional time-of-flight spectrometer with the detector kept in a shielding collimating the neutrons coming directly from the neutron producing target. This detector was placed at a distance of 5 m from the target, at an angle of 20° with respect to the direction of the incoming ion bursts. The portion of the neutron time spectrum corresponding to the neutrons emitted directly from the target was selected by a window discriminator to monitor the measurements. A functional block diagram of the electronics associated with the time-of-flight spectrometers is shown in Fig. 2.
The relative efficiency of the detectors was measured by comparing the yield of neutrons scattered on a hydrogeneous sample at several angles between 20° and 67.5° and the known n-p differential cross section [8]. The hydrogeneous sample was a polyethylene cylinder of 1.00 cm outside diameter, 0.60 cm inside diameter and 4.00 cm height. Its weight was 1.840 g and the content of hydrogen was $(14.31 \pm 0.06)\%$. The relative efficiencies of the detectors were measured twice, at the beginning and at the end of the scattering measurements on carbon. Within the experimental errors no variation of the efficiencies was found. The experimentally observed efficiency of detector 1, fitted with a semiempirical expression, is shown in Fig. 3.

The dimensions of the carbon samples used in the present measurements are shown in Table I. They were chosen in such a way that the corrections due to beam attenuation and multiple scattering do not change appreciably with the incident neutron energy.
The isotopic composition of the samples was 98.893% ^{12}C and 1.107% ^{13}C.

3. EXPERIMENTAL RESULTS

Angular distributions of neutrons scattered from carbon were measured at incident neutron energies between 0.50 and 2.00 MeV in energy steps of 50 keV. The scattered neutrons were detected between 20° and 150° with an angular spacing of 10°. The neutron scattering from the polyethylene sample was measured at + 30° and - 30° for the energies between 0.50 and 0.85 MeV and at + 40° and - 40° for

the energies between 0.90 and 2.00 MeV. In this way the presence of eventual experimental asymmetries of the neutron yield around zero degree was checked. No such asymmetry was observed within the experimental accuracy.

The absolute values of the differential cross section of carbon were determined comparatively to the H(n, n)H differential cross section. A typical time-of-flight spectrum of neutrons scattered from carbon is presented in Fig. 4.

A number of corrections were applied to the observed angular distribution data. The variation in the intensity of the $^{7}Li(p, n)^{7}Be$ and $T(p, n)^{3}He$ neutron yields as a function of angle and energy due to the finite target-to-sample geometry were taken into account.

The attenuation of the incoming neutron flux in the scattering samples and multiple scattering of neutrons within the polyethylene and carbon samples were also considered. The evaluation of the corrections were performed by a Monte Carlo Program (MAGGIE) in the version modified at the CBNM [10]. The applicability of this program is illustrated elsewhere [11-15] in several cases.

In evaluating the errors to the individual experimental points, the ones introduced by the counting statistics and those originating from the statistical nature of the Monte Carlo method were considered. A list of the error sources and their representative values is given in table II.

The differential elastic scattering angular distributions are shown in Figs. 5 to 35. The full circles represent the corrected experimental data in the laboratory system and the error bars are the total uncertainties.

A fit through the corrected differential scattering cross sections was made with a Legendre polynomial expansion of the form

$$\frac{d\sigma}{d\Omega}(\theta) = \sum_{L=0}^{4} B_L P_L(\cos\theta) \qquad (1)$$

The B_L-coefficients obtained from (1) were then fitted using an expression of the type

$$B_L(E) = \sum_{i=0}^{3} A_{L_i} E^i \qquad (2)$$

where the expansion on the right hand side of (2) was truncated after the second term for B_3 and B_4.

The values of $\sigma_{el}=4\pi B_o$ and of B_1 to B_4 obtained from the least squares fits (1) are given in table III together with their errors and are shown as full circles in Fig. 36 along with the fitted curves from (2). The numerical values of the measured differential elastic scattering cross sections are available at the ENEA Neutron Data Compilation Centre (France).

Using the $B_L(E)$-coefficients from (2) a consistent set of neutron differential cross section curves were calculated and are plotted as solid lines in Figs. 5 to 35. They are also shown in the form of a three dimensional plot in Fig. 37.

The explicit expression valid for σ_{el} in the energy region from 0.50 to 2.00 MeV is

$$\sigma_{el}(E) = (4.513 \pm 0.243) - (2.343 \pm 0.637)E + (0.465 \pm 0.520)E^2 + (0.012 \pm 0.133)E^3 \text{ barn},$$

where E is the incoming neutron energy in MeV. The overall error per point, including the computed error from the fitting procedure and errors from other sources is evaluated to about 3%.

In Fig. 38 the integrated elastic scattering cross sections from the present measurements are compared with the cross section results of other workers [4, 15-17]. The agreement between all these measurements, although made with different techniques, is good within the quoted errors.

ACKNOWLEDGEMENTS

The authors wish to thank Dr. J. Spaepen for his interest in this work. They are also grateful to the Sample Preparation and Metrology groups of CBNM for their collaboration in preparing and analysing the carbon samples. The help given by Mr. B. Jay during the performance of the experiment and by Dr. A. Crametz, Messrs. J. Leonard, R. Duchez and D. Bassetti from the accelerator staff is gratefully acknowledged.

REFERENCES

[1] K. Parker, AWRE Report n° 0-71/60 (1961).

[2] R. O. Lane, A. S. Langsdorf, Jr., J. E. Monahan, A. J. Elwyn, Annals of Physics 12 (1961) 135.

[3] J. E. Wills, Jr., J. K. Bair, H. O. Cohn, H. B. Willard, Phys. Rev. 109 (1958) 891.

[4] A. Langsdorf, Jr., R. O. Lane, and J. A. Monahan, ANL-5567 Rev. (1961).

[5] H. B. Willard, J. K. Bair, J. D. Kington, Phys. Rev. 98 (1955) 669.

[6] C. O. Muehlhause, S. D. Bloom, H. E. Wegner, G. N. Glasoe, Phys. Rev. 103 (1956) 720.

[7] W. L. Rogers, D. I. Garber, E. F. Shrader, Bull. Am. Phys. Soc. 6 (1961)61.

[8] J. L. Gammel, "Fast Neutron Physics", Part II (J. Marion and J. Fowler, Eds.) Interscience Publishers, Inc., New York (1963).

[9] Nuclear Data Sheets, Nuclear Data Group of the National Research Council, National Academy of Sciences.

[10] H. Schmidt and H. Horstmann, private communication.

[11] H.-H. Knitter and M. Coppola, EUR 3903. e (1968).

[12] H.-H. Knitter and M. Coppola, Z. Physik, 228 (1969) 286.

[13] M. Coppola and H.-H. Knitter, EUR 2798. e (1966).

[14] M. Coppola and H.-H. Knitter, Z. Physik, 232 (1970) 286.

[15] C. M. Huddleston, R. O. Lane, L. L. Lee, Jr., F. P. Mooring, Phys. Rev. 117 (1960) 1055, ANL-6111, (1960).

[16] K. M. Diment and C. A. Uttley, EANDC (UK) 94 AL.

[17] J. W. Meadows and J. F. Whalen, private communication (1969).

[18] R. O. Lane, A. Langsdorf, Jr., J. E. Monahan, A. J. Elwyn, ANL 6172 (1960).

FIGURE CAPTIONS

Fig. 1: Lay out of the experimental set-up.

Fig. 2: Block diagram of the electronic equipment.

Fig. 3: Relative efficiency of detector 1 measured at the beginning and at the end of the present experiment.

Fig. 4: Time-of-flight spectrum at E_{lab} = 1.10 MeV and θ_{lab} = 150°.

Fig. 5-35: Neutron differential elastic scattering cross-sections of carbon in the Lab.-system. Solid lines are calculated using the fitted B_L-coefficients from equation (2).

Fig. 36: Integrated neutron elastic scattering cross-sections of carbon and B_1 to B_4 coefficients. Full circles are the results of the present measurements and solid lines are the fits with equation (2). Triangles are the experimental values of Lane et al. [18].

Fig. 37: Three dimensional plot of neutron scattering angular distributions of carbon calculated using fitted B_L-coefficients.

Fig. 38: Comparison between σ_{el} results from the present measurements and those of other workers.

TABLE I

Carbon sample dimensions				Neutron energy region (MeV)
Outside diameter (cm)	Inside diameter (cm)	Height (cm)	Weight (g)	
2.00	0.86	3.505	15.462	0.50 - 1.25
1.41	0.00	3.500	9.375	1.30 - 1.70
1.72	0.00	3.500	13.897	1.75 - 2.00

TABLE II

Sources of errors for the differential elastic cross sections and their representative relative errors

Sources of errors	Errors (%)
Detector efficiency	2.00
Total n-p scattering cross section	0.50
Counting statistics on H	1.00
Flux factor in C-sample:	
1) due to fluctuations in flux calculations	0.45
2) due to uncertainties of σ_T	0.70
Multiple scattering correction in carbon	0.70
α-factor in CH_2	1.00
Hydrogen content in CH_2	0.5
Sum of the errors	2.8
Counting statistics on carbon	1 - 3

TABLE III

Integrated elastic scattering cross sections and Legendre polynomial coefficients of carbon in the laboratory system

E_{Lab} [MeV]	$\sigma_{el} \pm \Delta\sigma_{el}$ [mb]	$B_1 \pm \Delta B_1$ [mb/sr]	$B_2 \pm \Delta B_2$ [mb/sr]	$B_3 \pm \Delta B_3$ [mb/sr]	$B_4 \pm \Delta B_4$ [mb/sr]
0.50	3304 ± 97	121.2 ± 5.1	26.8 ± 5.1	5.8 ± 6.3	-5.1 ± 7.7
0.55	3385 ± 100	111.1 ± 5.2	7.9 ± 5.8	0.7 ± 7.2	4.9 ± 8.8
0.60	3312 ± 96	117.6 ± 3.9	9.7 ± 3.0	12.4 ± 3.7	18.4 ± 4.5
0.65	3291 ± 95	102.8 ± 3.8	16.4 ± 6.4	14.7 ± 7.8	-3.3 ± 9.7
0.70	3085 ± 94	93.0 ± 6.3	9.3 ± 8.0	10.5 ± 10.0	-1.5 ± 12.1
0.75	3059 ± 89	107.9 ± 4.3	22.2 ± 4.3	7.3 ± 5.3	-4.3 ± 6.5
0.80	3017 ± 87	90.7 ± 3.7	29.7 ± 3.8	2.2 ± 4.6	-0.4 ± 5.7
0.85	2882 ± 84	93.0 ± 4.0	26.0 ± 4.1	-2.3 ± 5.2	-8.4 ± 0.3
0.90	2819 ± 83	89.3 ± 4.2	19.6 ± 4.8	1.5 ± 5.7	1.9 ± 7.6
0.95	2724 ± 79	89.9 ± 3.7	24.0 ± 3.6	12.2 ± 4.5	-5.9 ± 5.6
1.00	2655 ± 78	81.6 ± 4.6	30.7 ± 5.8	-4.2 ± 6.5	4.9 ± 7.5
1.05	2662 ± 76	85.4 ± 3.0	22.4 ± 2.5	-4.4 ± 3.1	-1.9 ± 3.9
1.10	2399 ± 70	77.6 ± 3.3	21.2 ± 3.5	6.8 ± 4.4	2.9 ± 5.3
1.15	2429 ± 72	75.5 ± 3.7	19.0 ± 4.3	7.3 ± 5.4	10.4 ± 6.5
1.20	2271 ± 65	67.6 ± 2.7	10.2 ± 2.7	1.4 ± 3.4	-1.3 ± 4.1
1.25	2299 ± 68	67.6 ± 3.4	18.4 ± 3.9	7.8 ± 4.9	4.0 ± 6.3
1.30	2291 ± 68	73.7 ± 3.6	18.4 ± 4.0	2.1 ± 5.0	-10.6 ± 6.3
1.35	2290 ± 67	69.6 ± 3.3	26.9 ± 3.8	7.0 ± 4.6	3.7 ± 5.7
1.40	2194 ± 64	73.6 ± 3.1	25.7 ± 3.1	-1.7 ± 3.8	-0.5 ± 4.7
1.45	2138 ± 63	65.2 ± 3.3	27.1 ± 3.8	10.6 ± 4.6	0.4 ± 5.7
1.50	2117 ± 61	58.3 ± 2.7	19.3 ± 2.9	11.6 ± 3.6	-3.4 ± 4.4
1.55	2023 ± 59	62.9 ± 2.7	22.7 ± 2.8	6.6 ± 3.6	0.5 ± 4.5
1.60	2017 ± 58	54.7 ± 2.4	28.2 ± 2.5	8.1 ± 2.9	0.0 ± 3.4
1.65	1978 ± 60	56.3 ± 3.5	29.2 ± 4.3	2.4 ± 5.3	1.7 ± 6.5
1.70	1931 ± 57	52.2 ± 3.2	18.6 ± 4.5	5.4 ± 5.1	-15.0 ± 6.3
1.75	1935 ± 55	54.7 ± 2.2	29.8 ± 2.1	6.3 ± 2.5	-1.3 ± 3.1
1.80	1876 ± 53	52.9 ± 2.3	32.0 ± 2.4	4.8 ± 3.0	-2.7 ± 3.6
1.85	1849 ± 53	48.5 ± 2.3	32.6 ± 2.5	7.6 ± 3.0	-1.9 ± 3.8
1.90	1826 ± 52	49.5 ± 2.5	32.3 ± 2.9	14.4 ± 3.2	-5.0 ± 4.0
1.95	1806 ± 54	48.1 ± 3.0	36.0 ± 4.3	16.2 ± 4.9	-8.4 ± 5.7
2.00	1769 ± 53	41.0 ± 3.1	39.8 ± 3.9	-11.2 ± 4.6	-0.4 ± 5.7

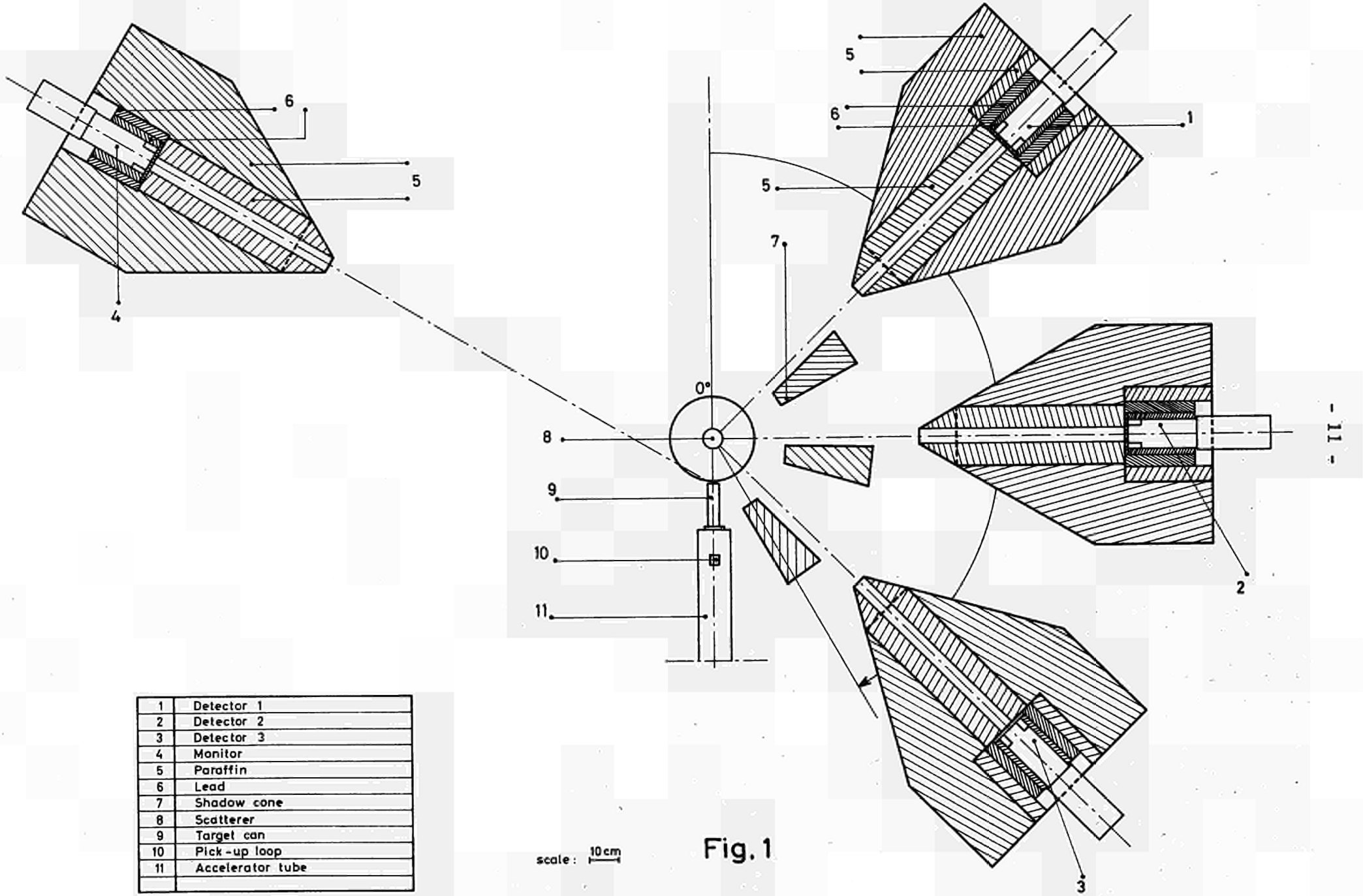

1	Detector 1
2	Detector 2
3	Detector 3
4	Monitor
5	Paraffin
6	Lead
7	Shadow cone
8	Scatterer
9	Target can
10	Pick-up loop
11	Accelerator tube

scale: 10 cm

Fig. 1

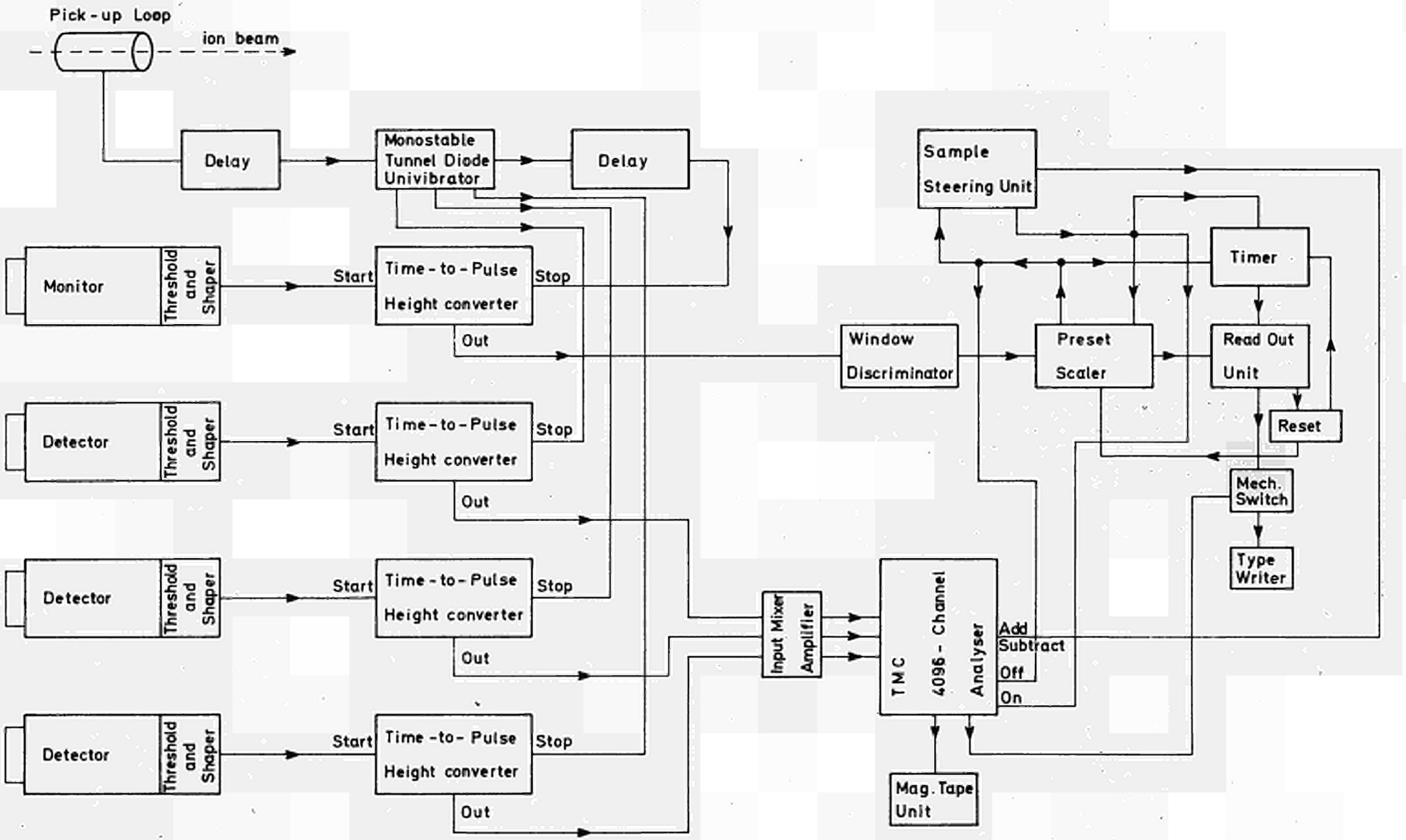
Pick-up Loop
ion beam
Delay
Monostable Tunnel Diode Univibrator
Delay
Sample Steering Unit
Timer
Monitor
Threshold and Shaper
Start
Time-to-Pulse Height converter
Stop
Out
Window Discriminator
Preset Scaler
Read Out Unit
Reset
Detector
Threshold and Shaper
Start
Time-to-Pulse Height converter
Stop
Out
Mech. Switch
Type Writer
Detector
Threshold and Shaper
Start
Time-to-Pulse Height converter
Stop
Out
Input Mixer Amplifier
TMC 4096-Channel Analyser
Add
Subtract
Off
On
Detector
Threshold and Shaper
Start
Time-to-Pulse Height converter
Stop
Out
Mag. Tape Unit

Fig. 2

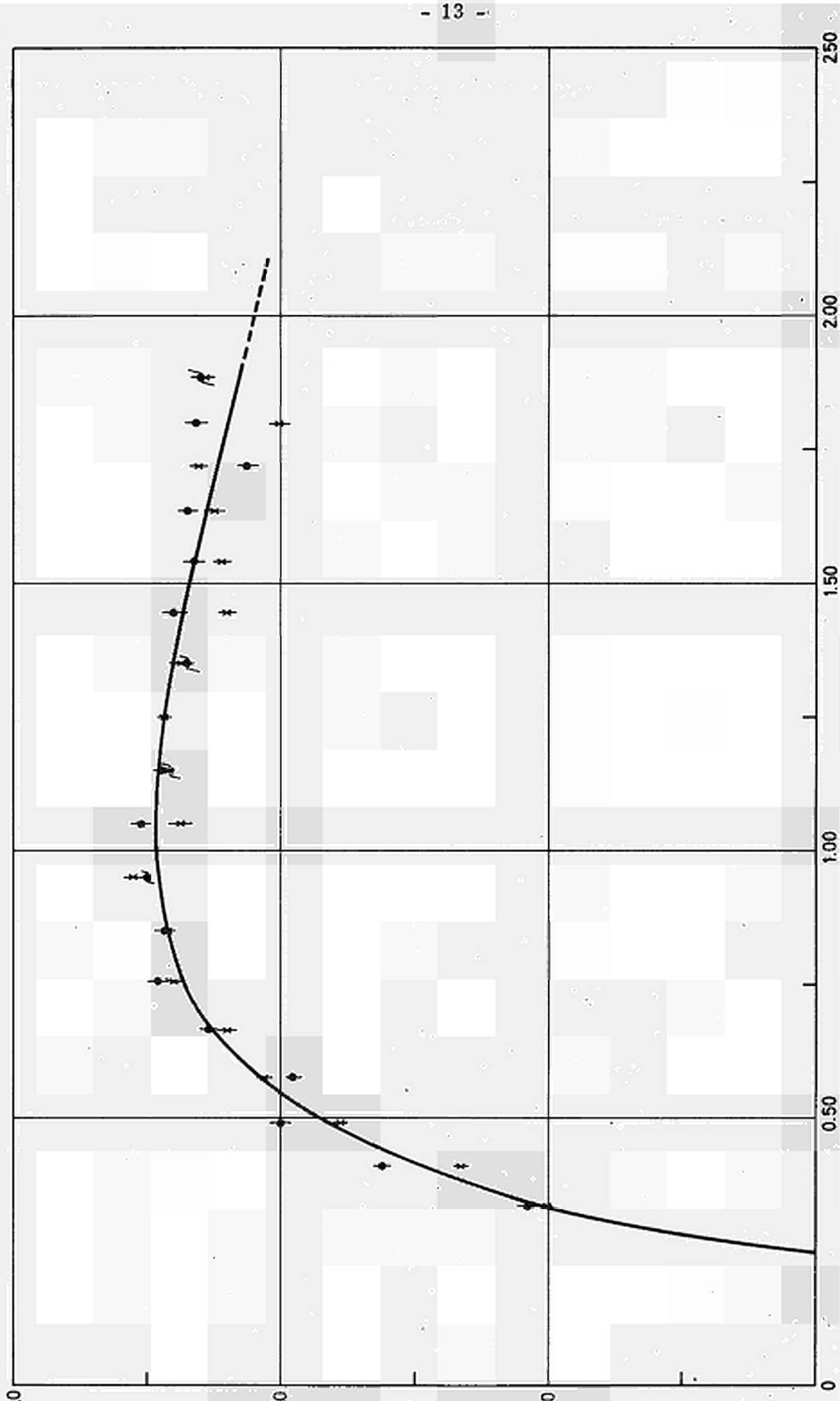
Efficiency of counter 1 [arbitrary units]
12.0
8.0
4.0
0
0.50
1.00
1.50
2.00
250
E_{lab}[MeV]

Fig.3

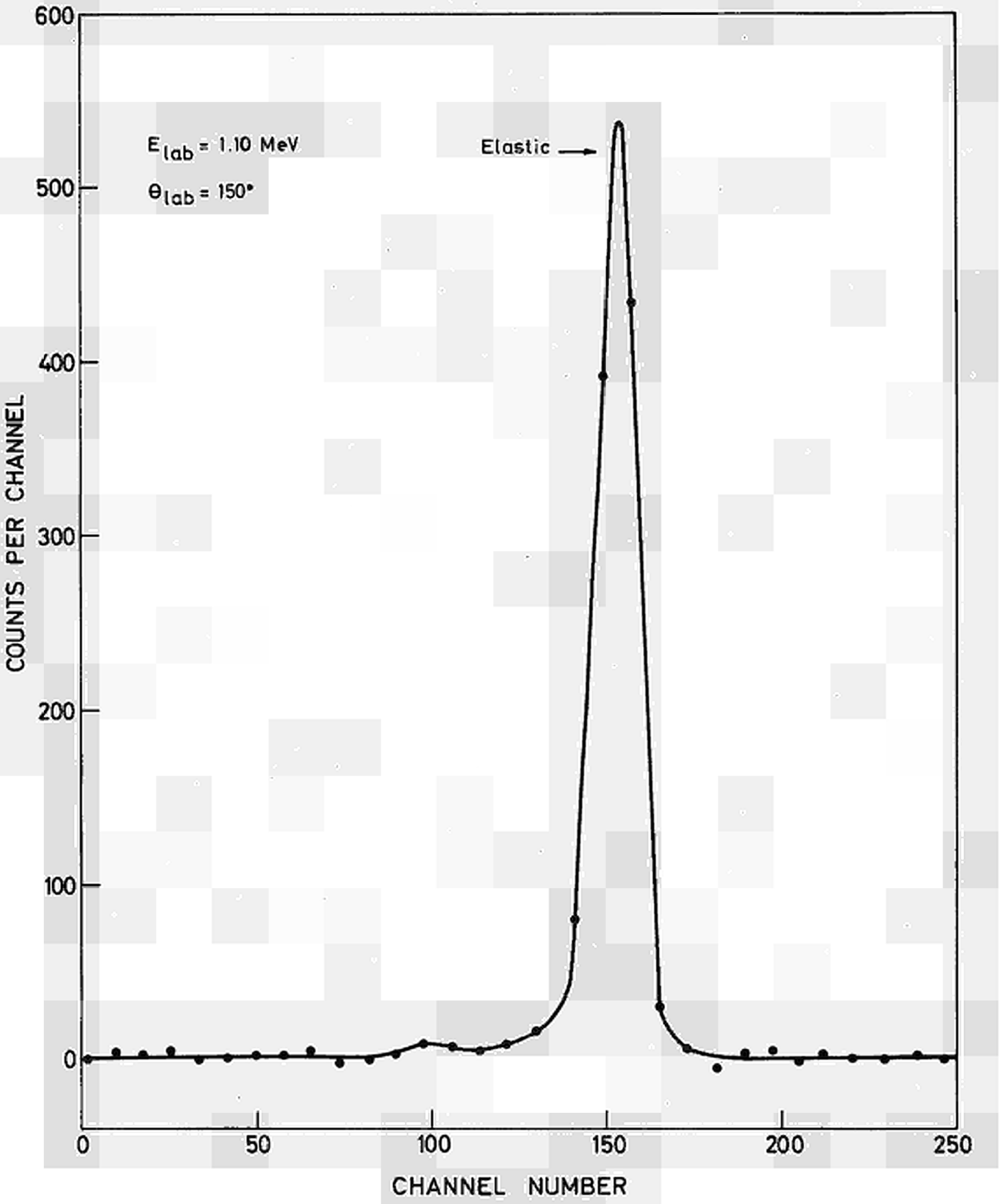
600
500
400
300
200
100
0
E_{lab} = 1.10 MeV
θ_{lab} = 150°
Elastic
COUNTS PER CHANNEL
0
50
100
150
200
250
CHANNEL NUMBER

Fig. 4

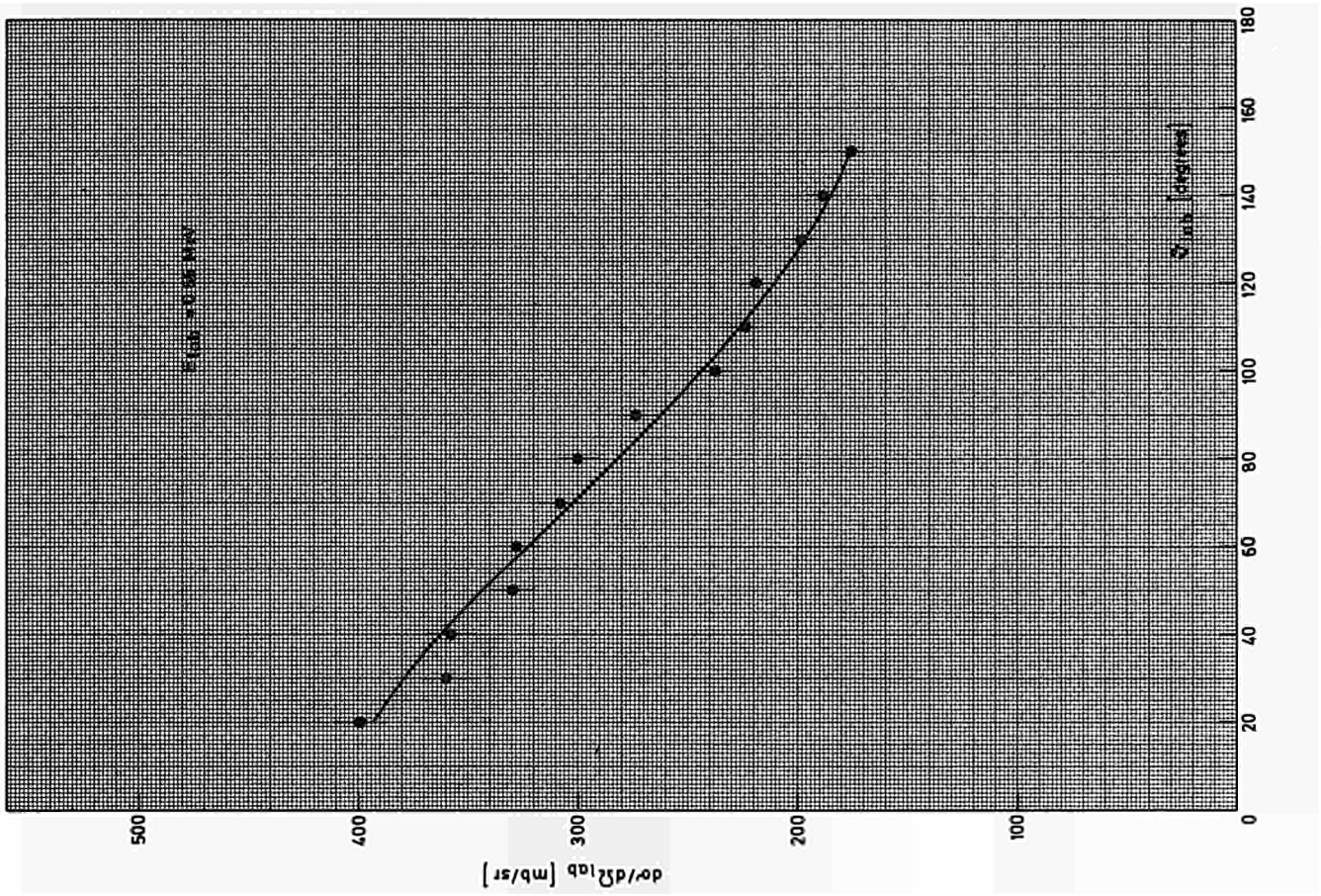
dσ/dΩlab [mb/sr]
500
400
300
200
100
0
20
40
60
80
100
120
140
160
180
θlab [degrees]

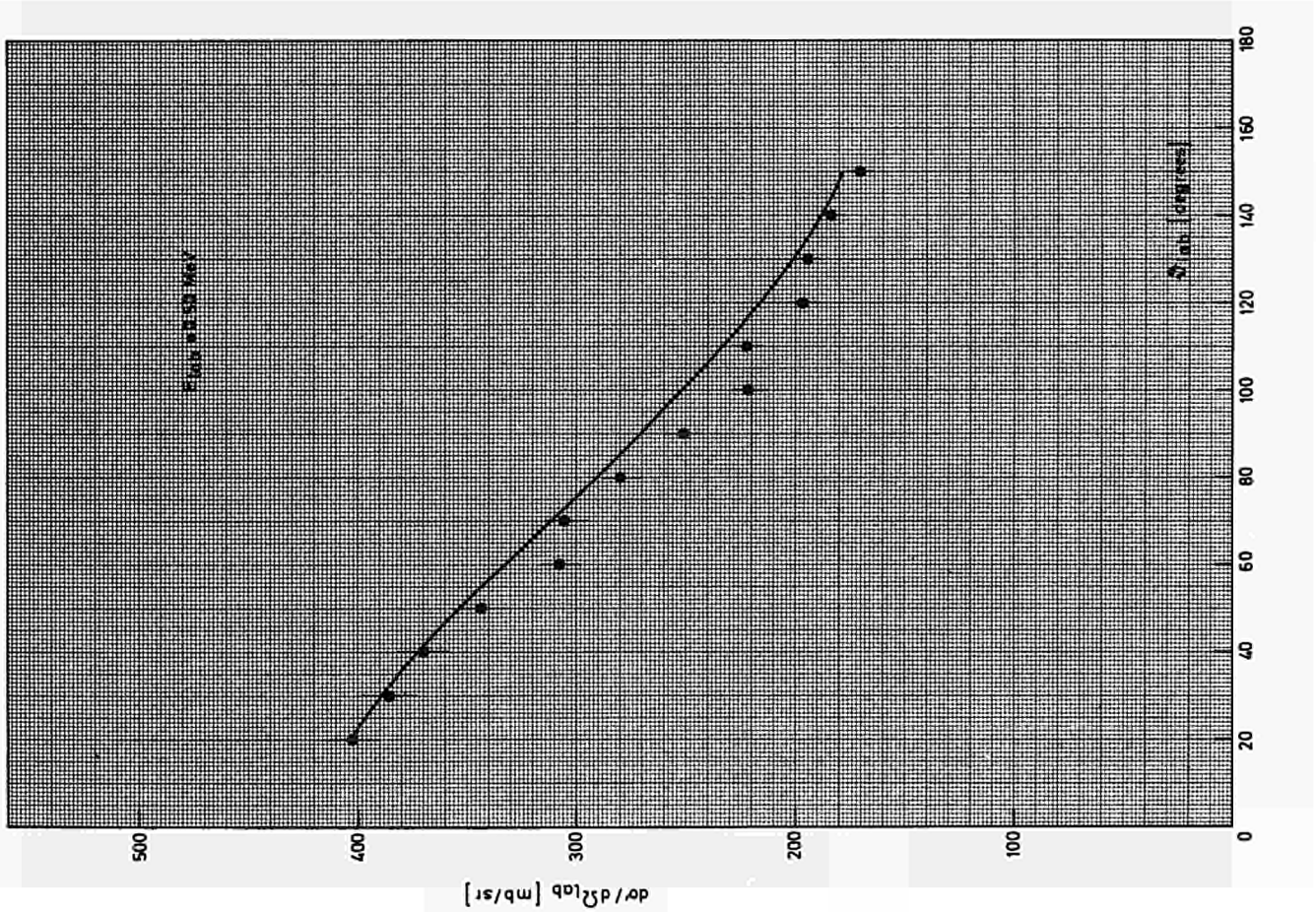
dσ/dΩlab [mb/sr]
500
400
300
200
100
0
20
40
60
80
100
120
140
160
180
θlab [degrees]

E_{lab} = 0.60 MeV
$d\sigma / d\Omega_{lab}$ [mb/sr]
ϑ_{lab} [degrees]
0
20
40
60
80
100
120
140
160
180
100
200
300
400
500

E_{lab} = 2.65 MeV
$d\sigma / d\Omega_{lab}$ [mb/sr]
ϑ_{lab} [degrees]
0
20
40
60
80
100
120
140
160
180
100
200
300
400
500

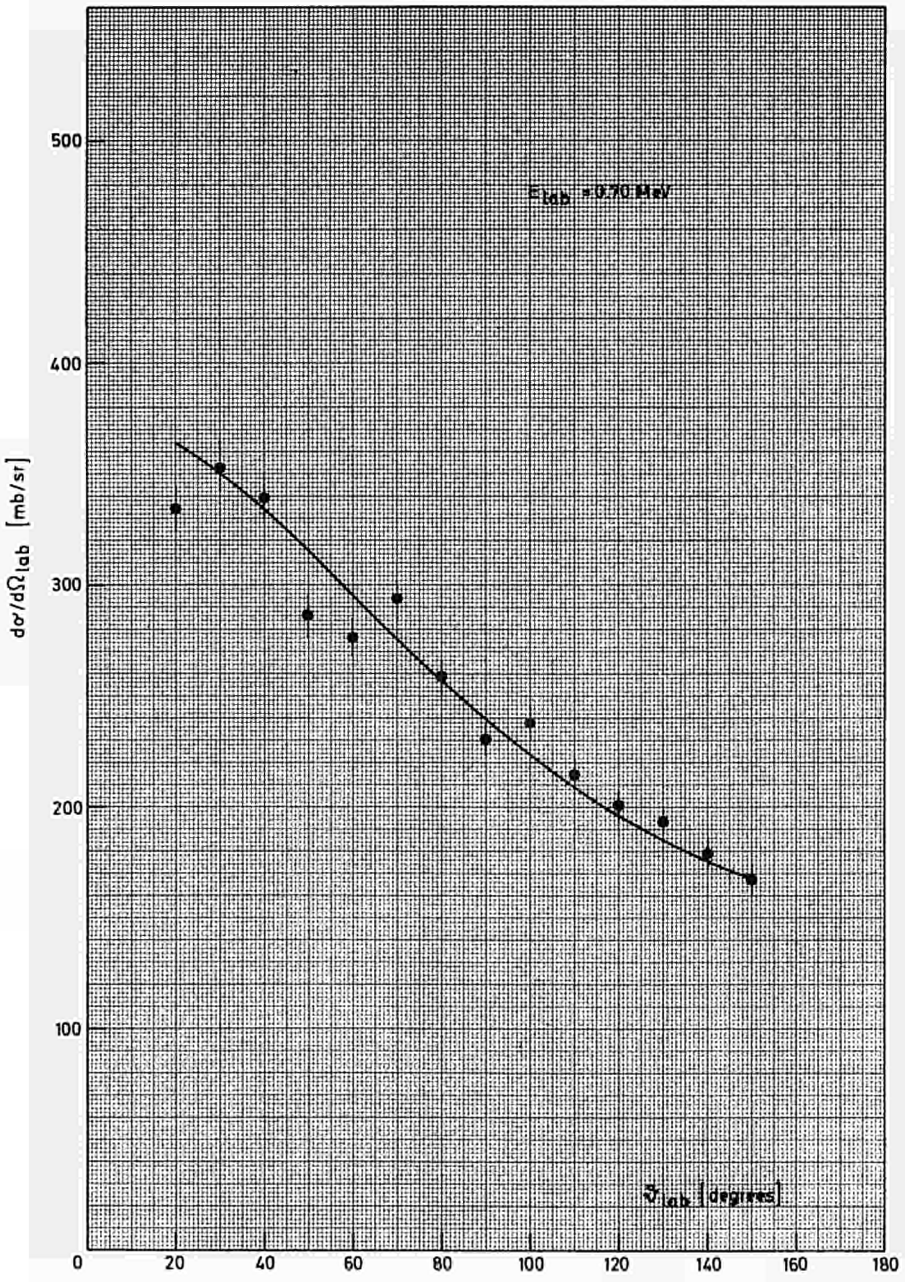
E_{lab} = 0.70 MeV
$d\sigma/d\Omega_{lab}$ [mb/sr]
ϑ_{lab} [degrees]
0
20
40
60
80
100
120
140
160
180
100
200
300
400
500

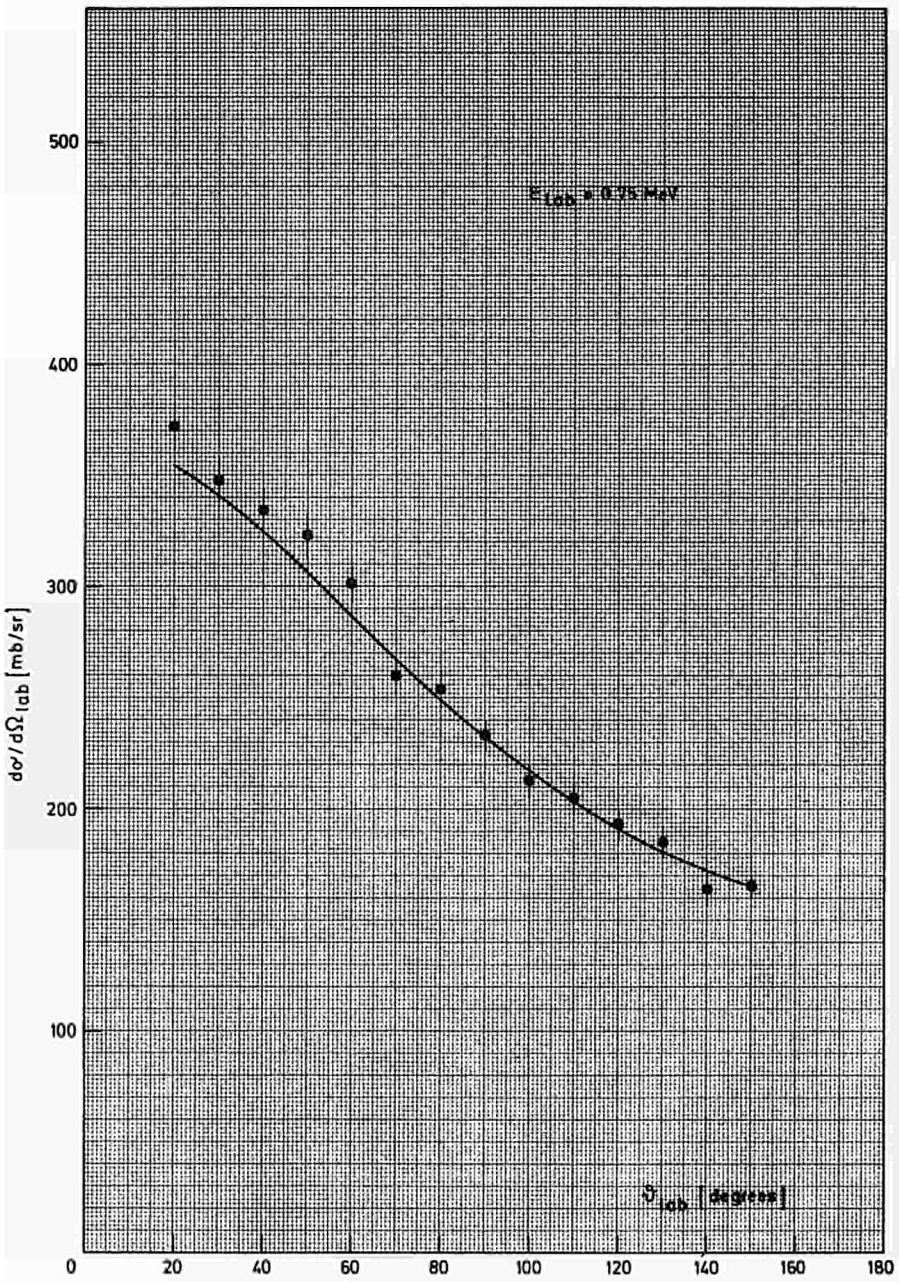
E_{lab} = 0.75 MeV
$d\sigma/d\Omega_{lab}$ [mb/sr]
ϑ_{lab} [degrees]
0
20
40
60
80
100
120
140
160
180
100
200
300
400
500

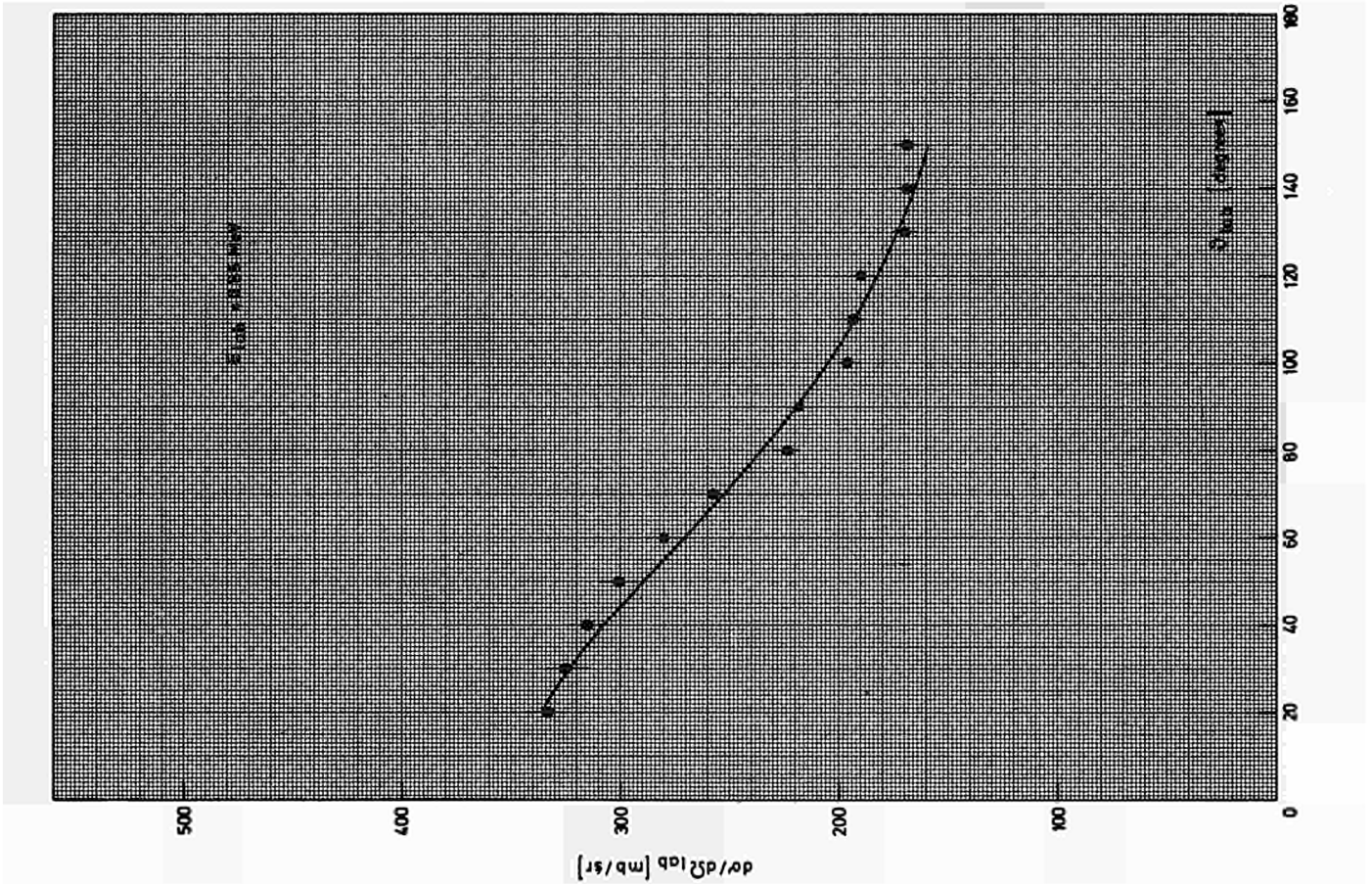
dσ/dΩlab [mb/sr]
500
400
300
200
100
0
20
40
60
80
100
120
140
160
180
θlab [degrees]

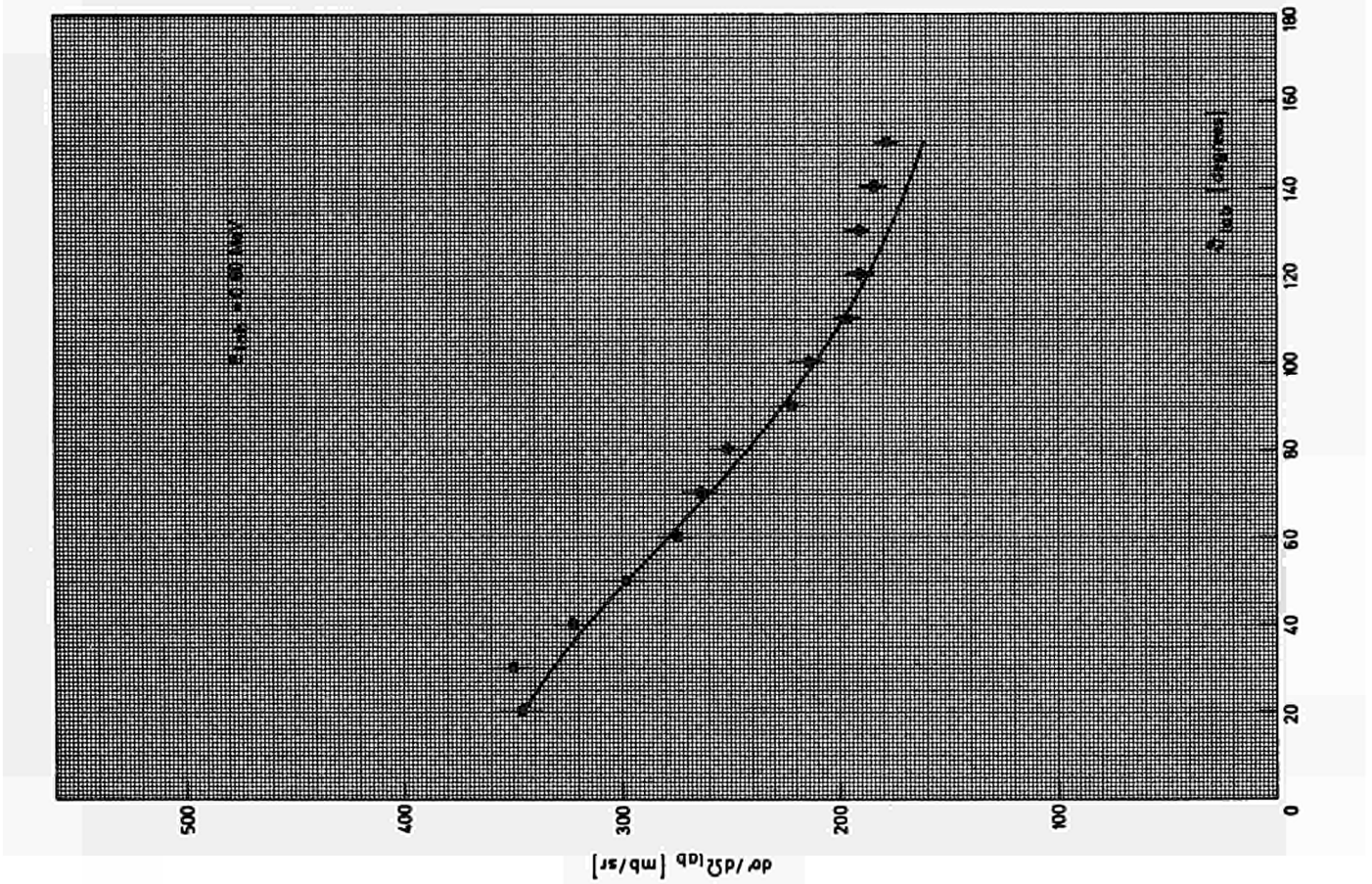
dσ/dΩlab [mb/sr]
500
400
300
200
100
0
20
40
60
80
100
120
140
160
180
θlab [degrees]

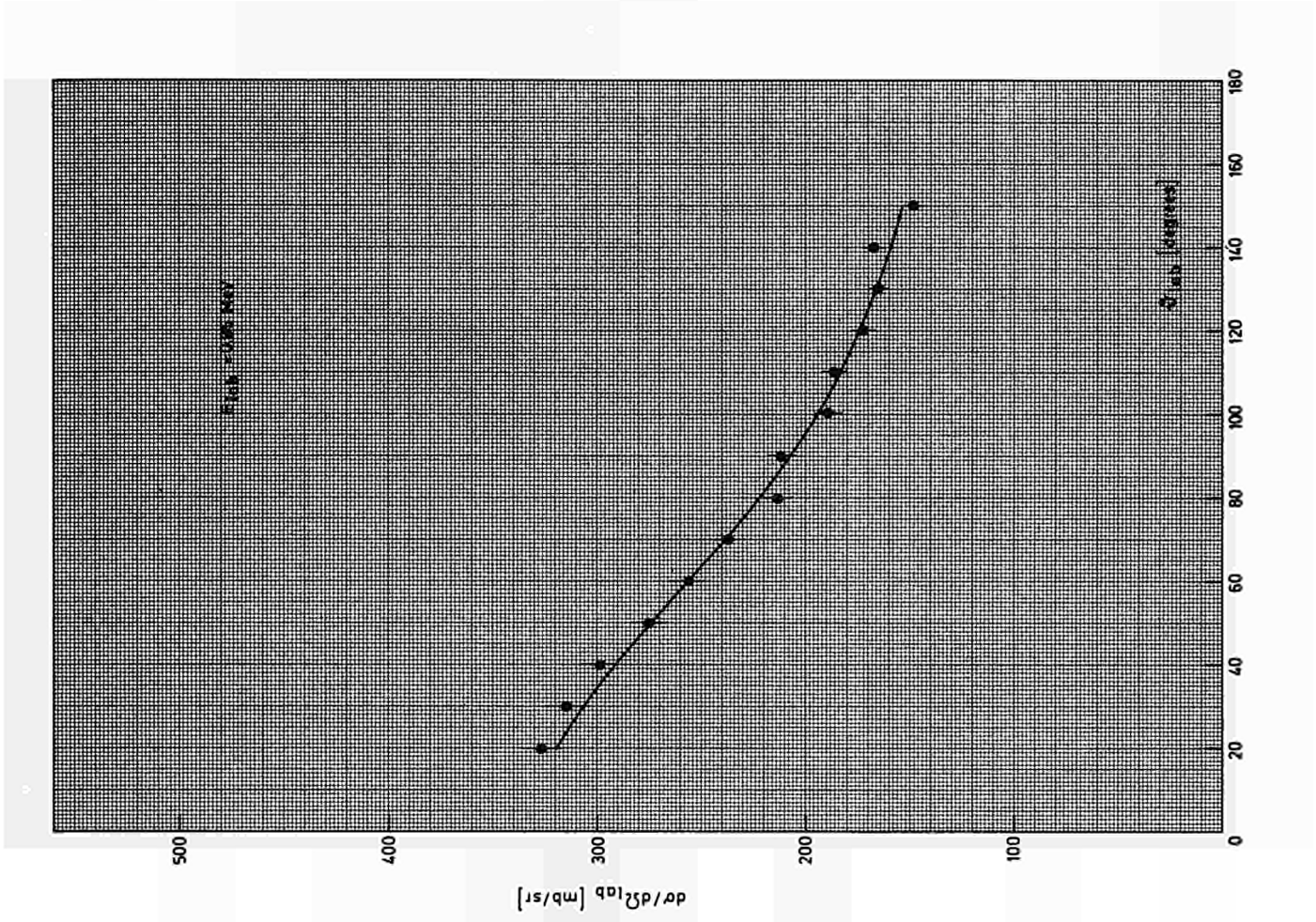
E_{lab} = 1.00 MeV
ϑ_{lab} [degrees]
$d\sigma/d\Omega_{lab}$ [mb/sr]
0
20
40
60
80
100
120
140
160
180
100
200
300
400
500

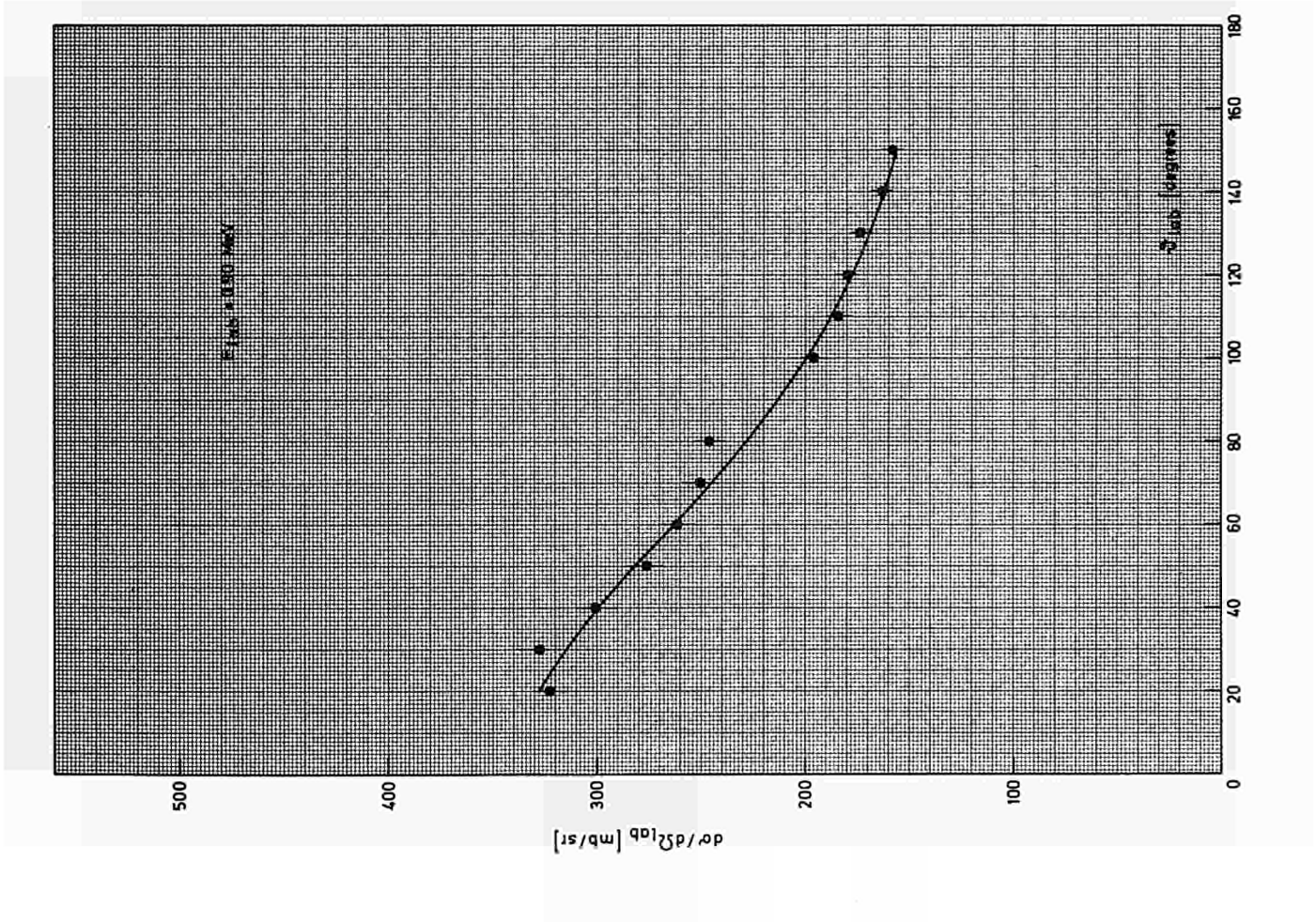
E_{lab} = 0.80 MeV
ϑ_{lab} [degrees]
$d\sigma/d\Omega_{lab}$ [mb/sr]
0
20
40
60
80
100
120
140
160
180
100
200
300
400
500

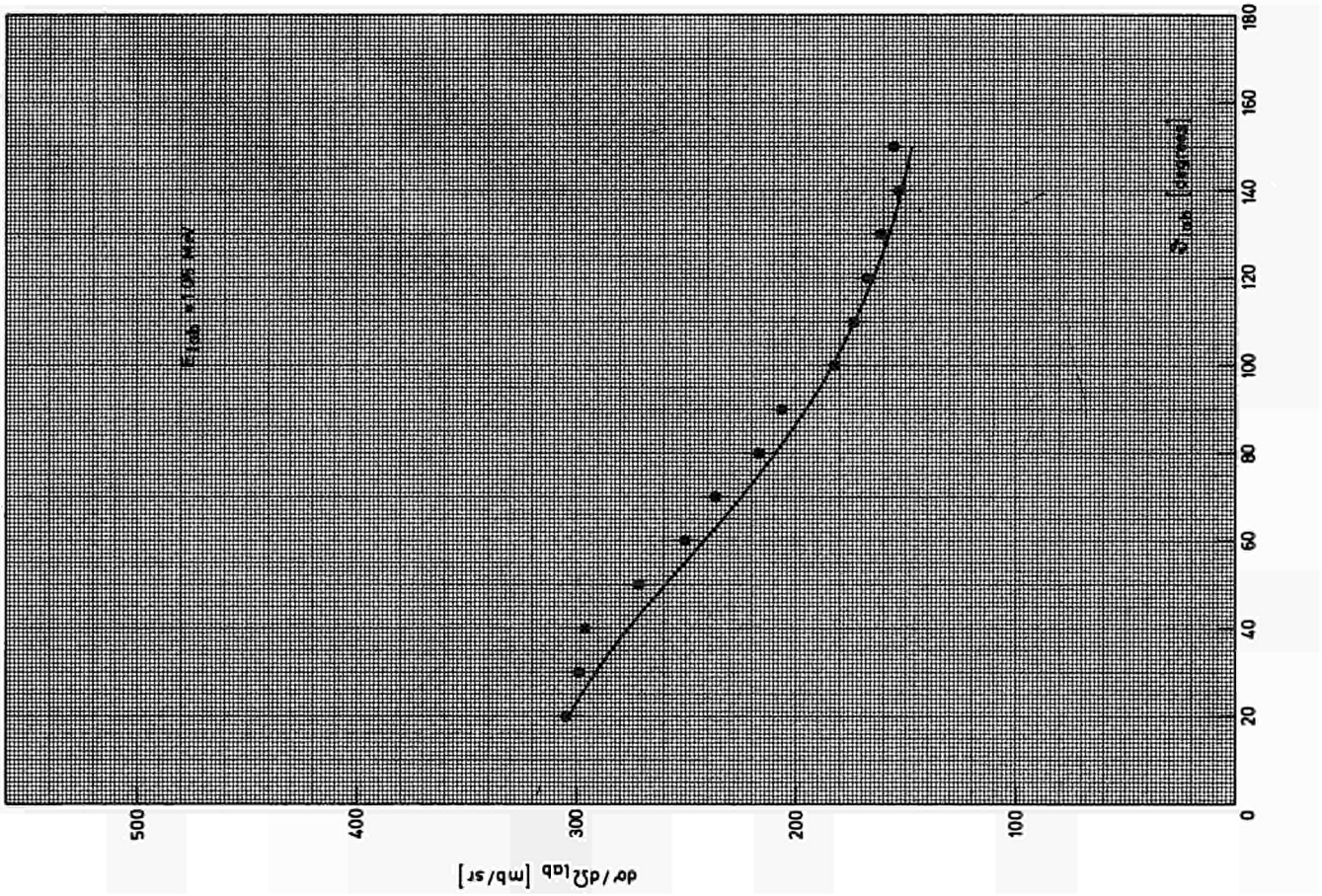
dσ/dΩlab [mb/sr]
0
100
200
300
400
500
20
40
60
80
100
120
140
160
180

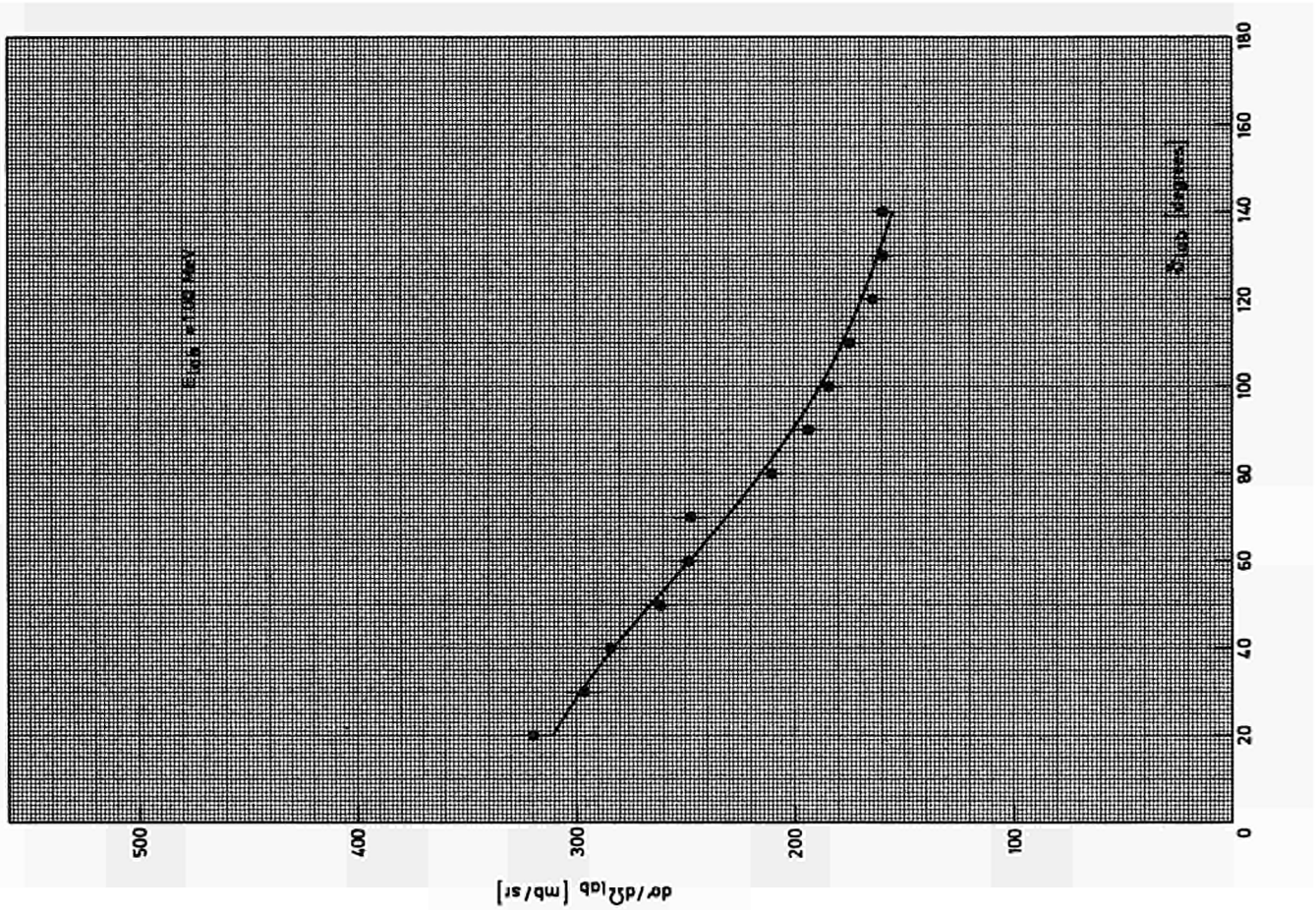
dσ/dΩlab [mb/sr]
0
100
200
300
400
500
20
40
60
80
100
120
140
160
180

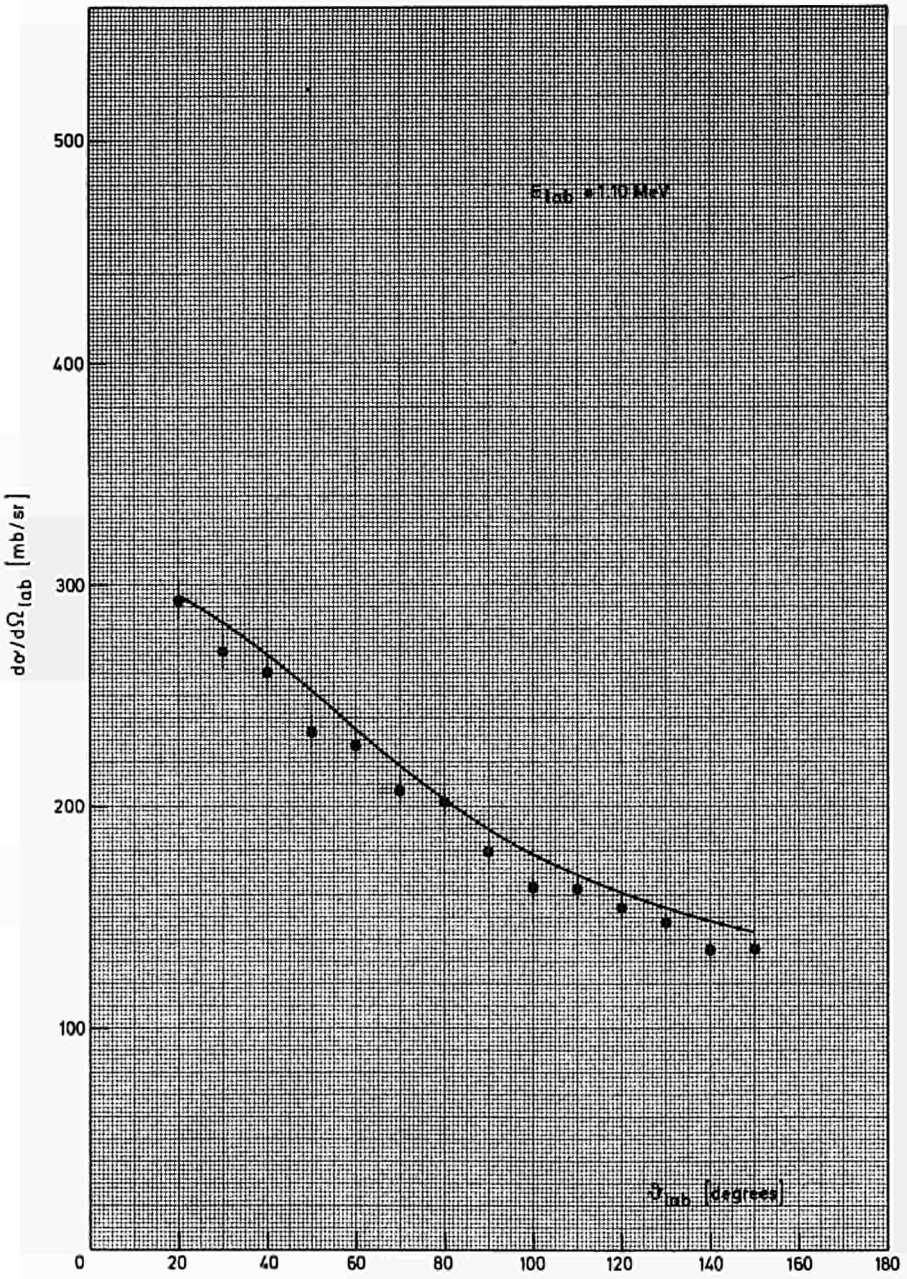
E_{lab} = 1.10 MeV
$d\sigma/d\Omega_{lab}$ [mb/sr]
ϑ_{lab} [degrees]
0
20
40
60
80
100
120
140
160
180
100
200
300
400
500

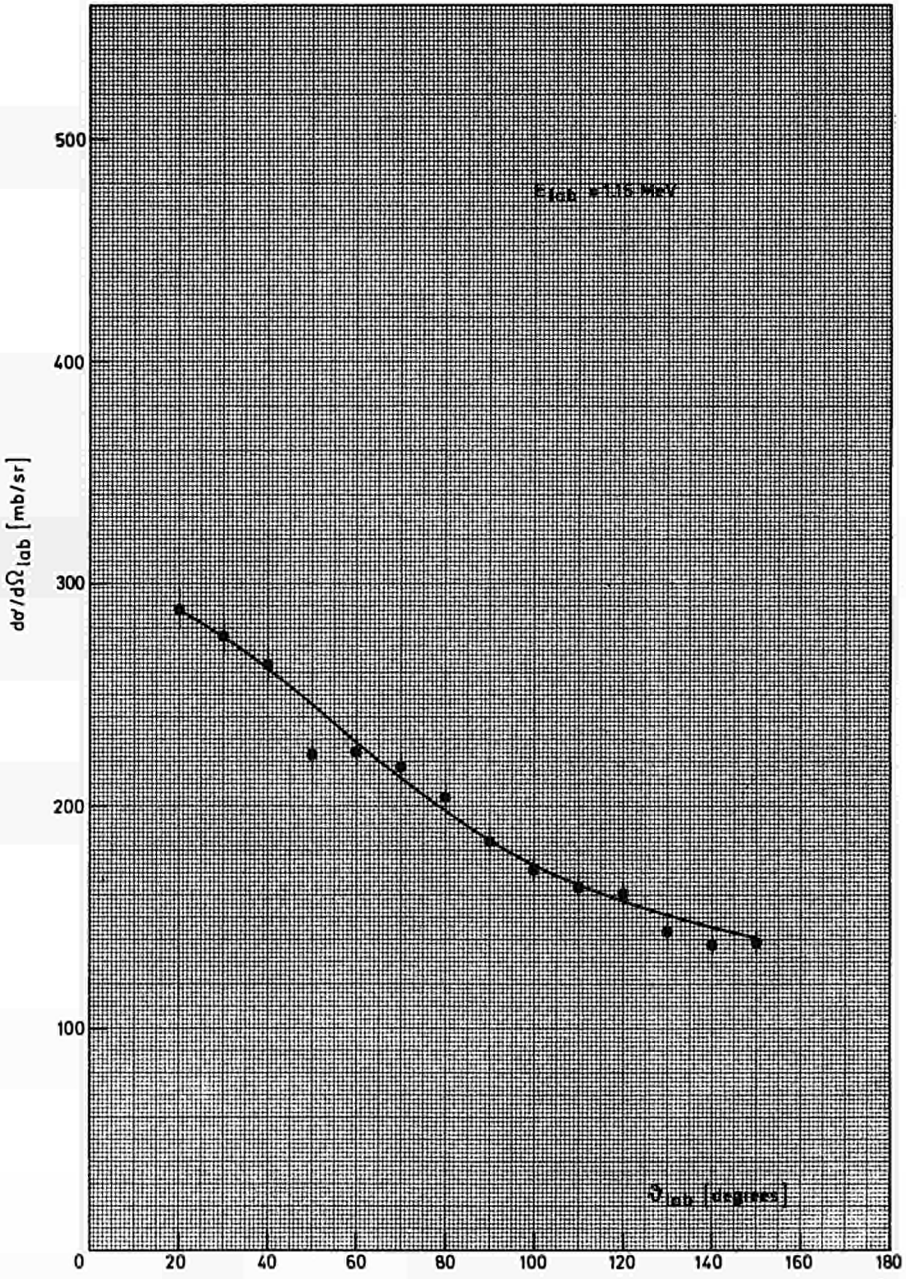
E_{lab} = 1.15 MeV
$d\sigma/d\Omega_{lab}$ [mb/sr]
ϑ_{lab} [degrees]
0
20
40
60
80
100
120
140
160
180
100
200
300
400
500

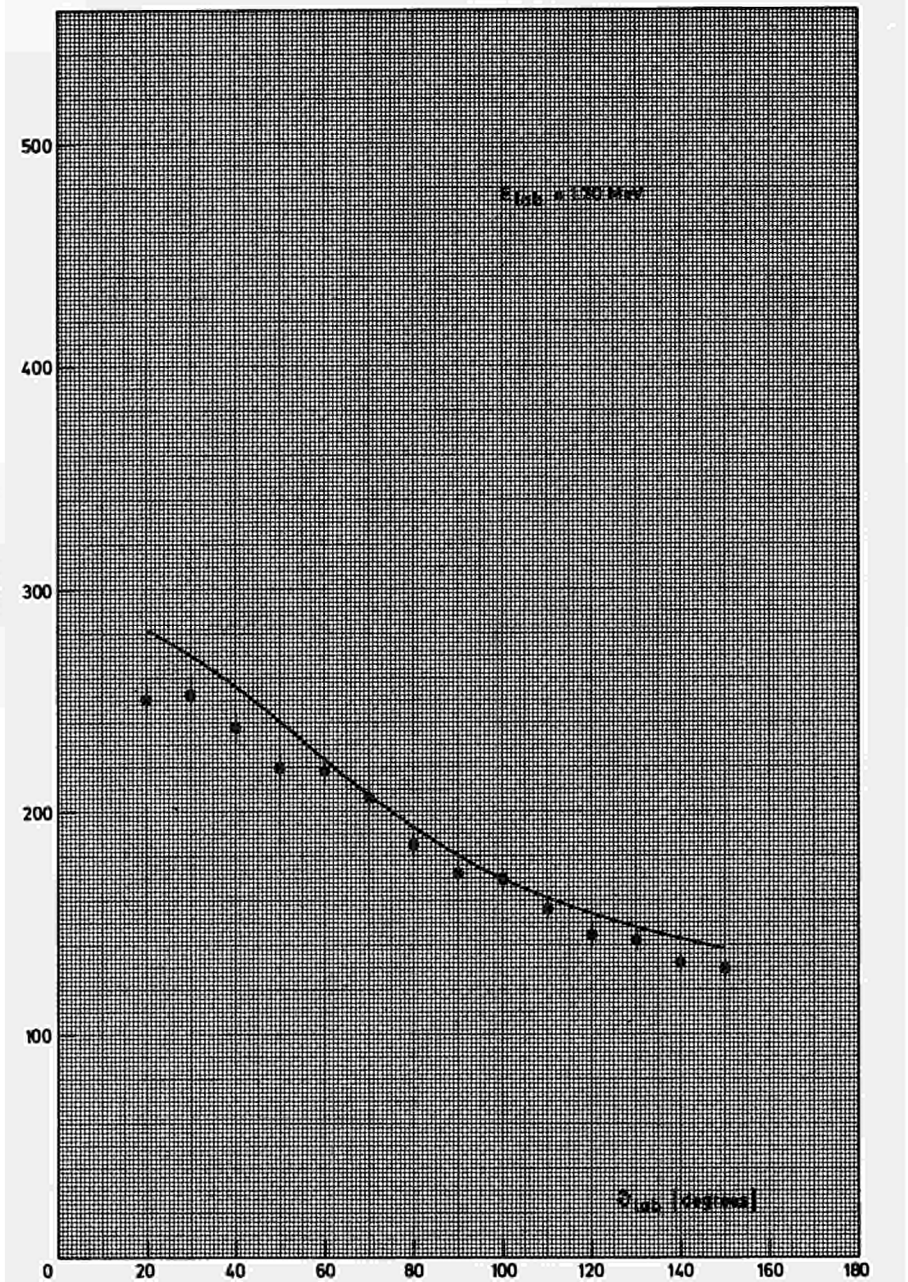
E_{lab} = 150 MeV
$d\sigma/d\Omega_{lab}$ [mb/sr]
ϑ_{lab} [degrees]
0
20
40
60
80
100
120
140
160
180
100
200
300
400
500

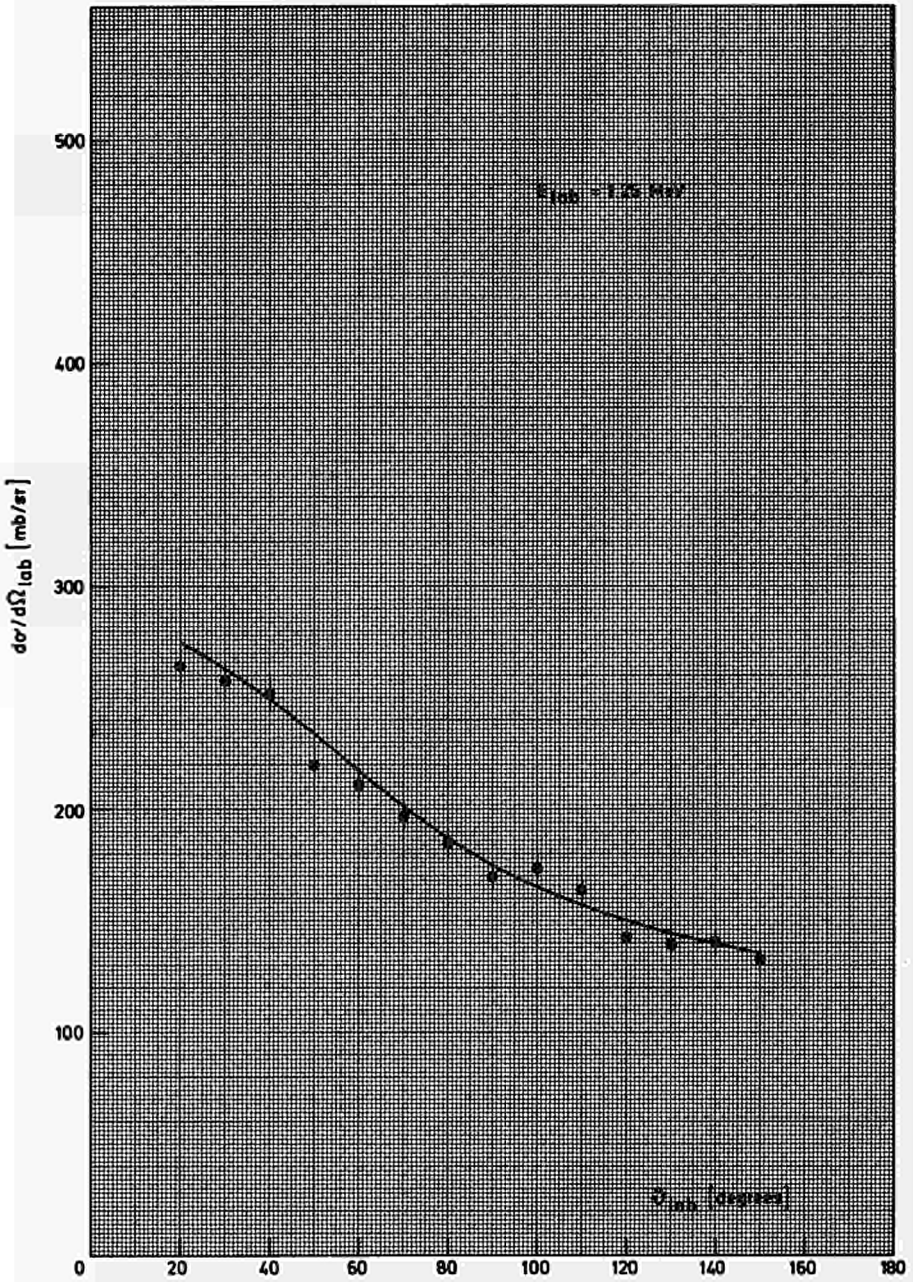
E_{lab} = 135 MeV
$d\sigma/d\Omega_{lab}$ [mb/sr]
ϑ_{lab} [degrees]
0
20
40
60
80
100
120
140
160
180
100
200
300
400
500

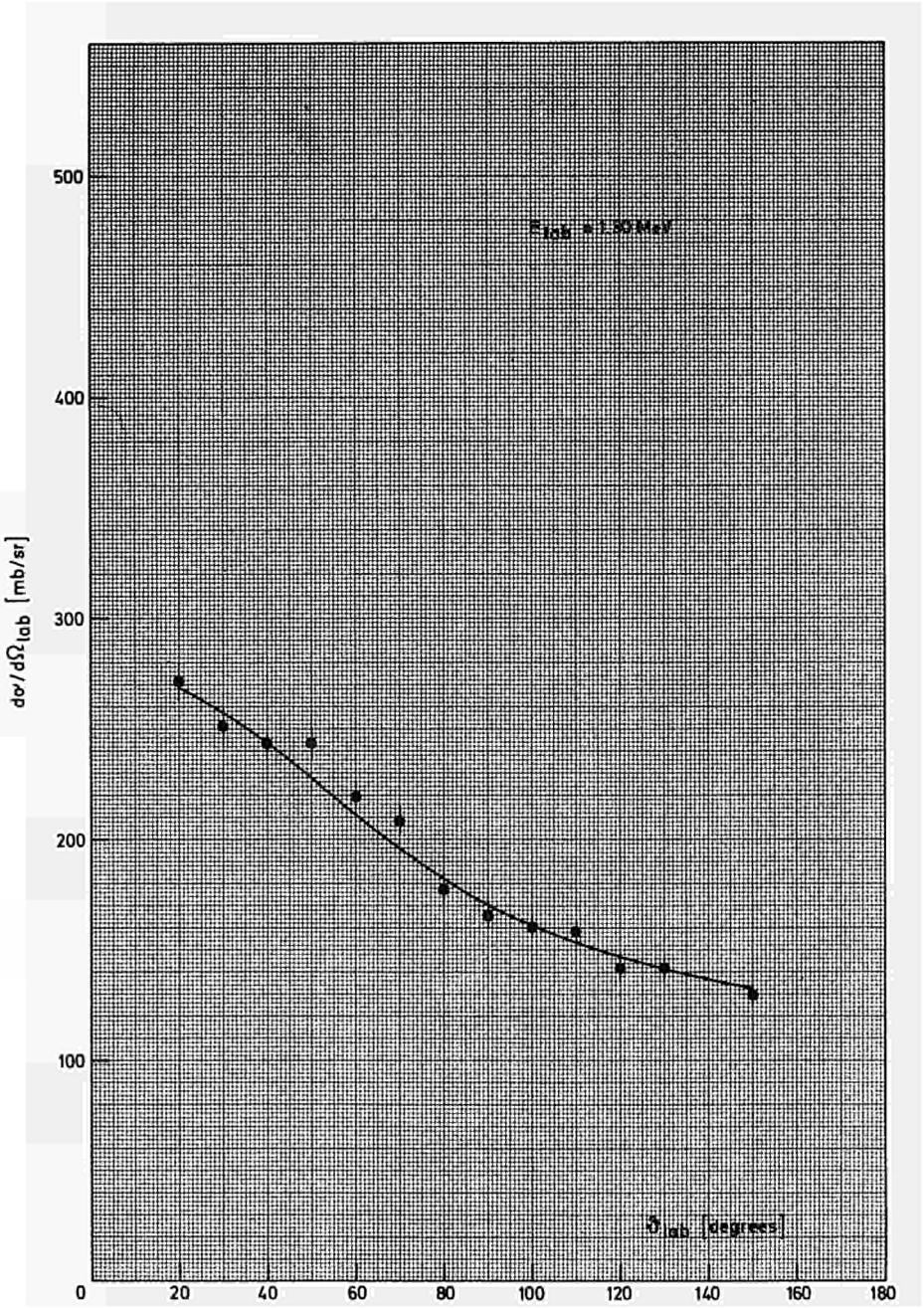
E_{lab} = 1.50 MeV
$d\sigma/d\Omega_{lab}$ [mb/sr]
ϑ_{lab} [degrees]
0
100
200
300
400
500
0
20
40
60
80
100
120
140
160
180

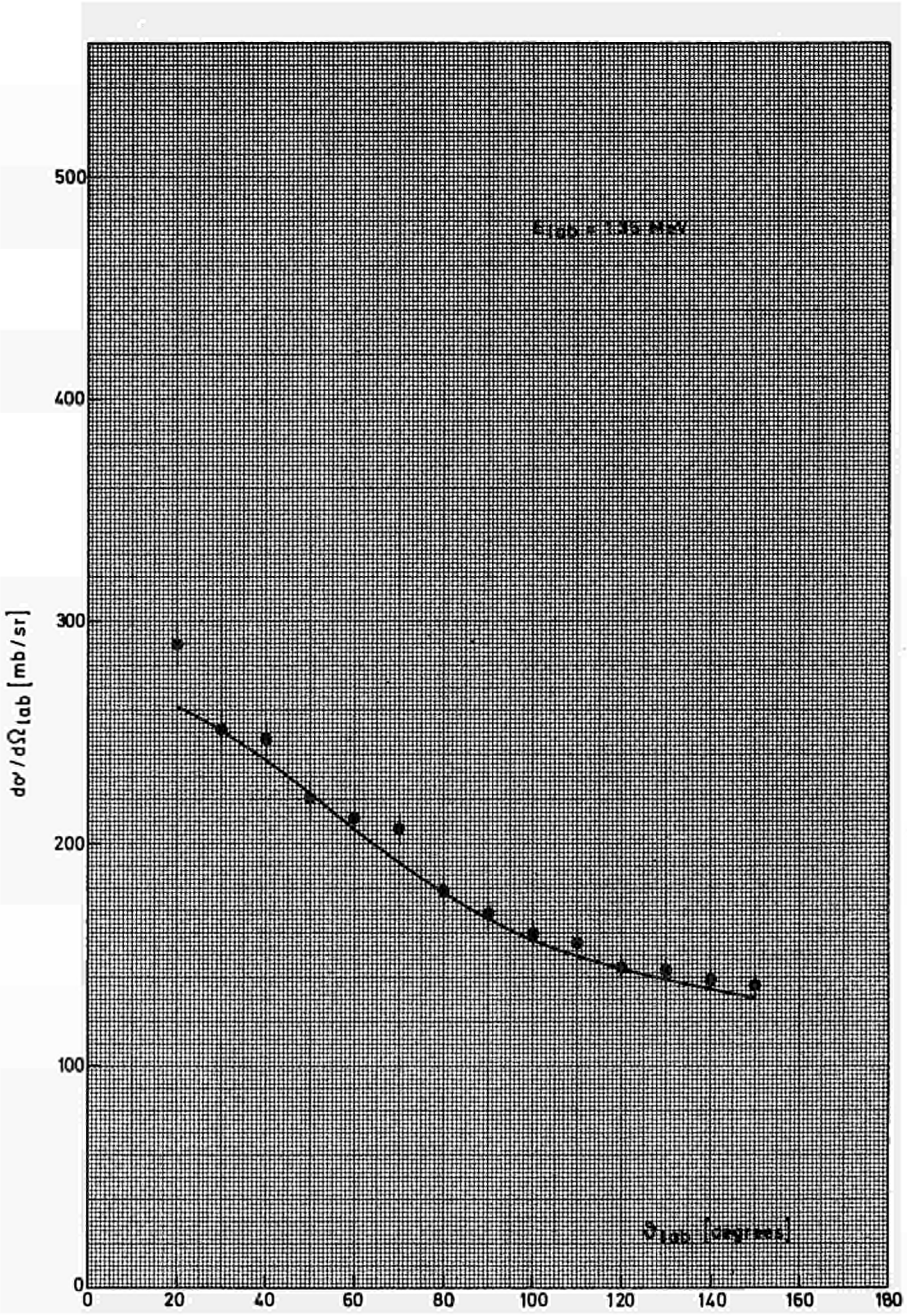
E_{lab} = 1.35 MeV
$d\sigma/d\Omega_{lab}$ [mb/sr]
ϑ_{lab} [degrees]
0
100
200
300
400
500
0
20
40
60
80
100
120
140
160
180

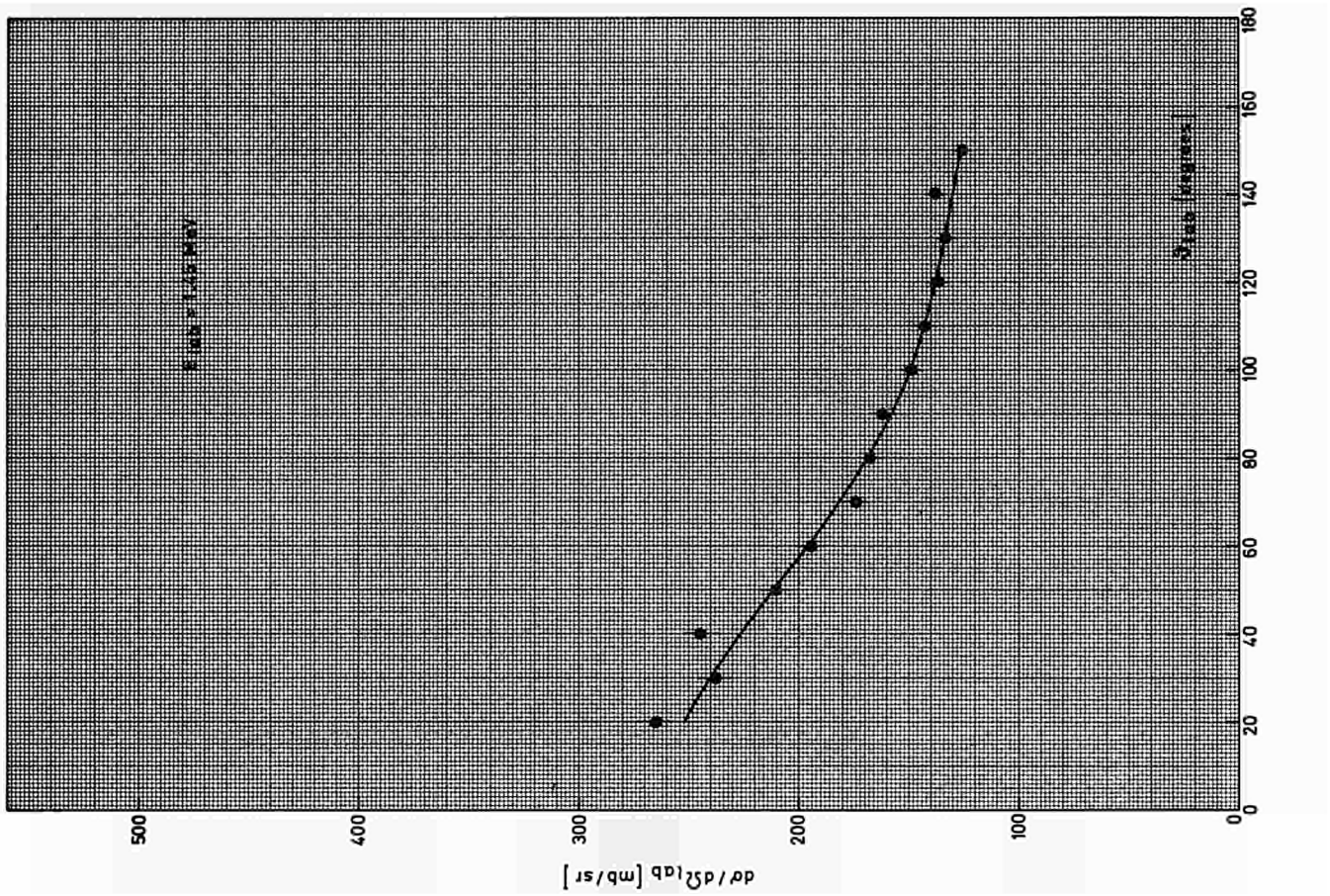
dσ/dΩ_lab [mb/sr]
0
100
200
300
400
500
0
20
40
60
80
100
120
140
160
180
θ_lab [degrees]

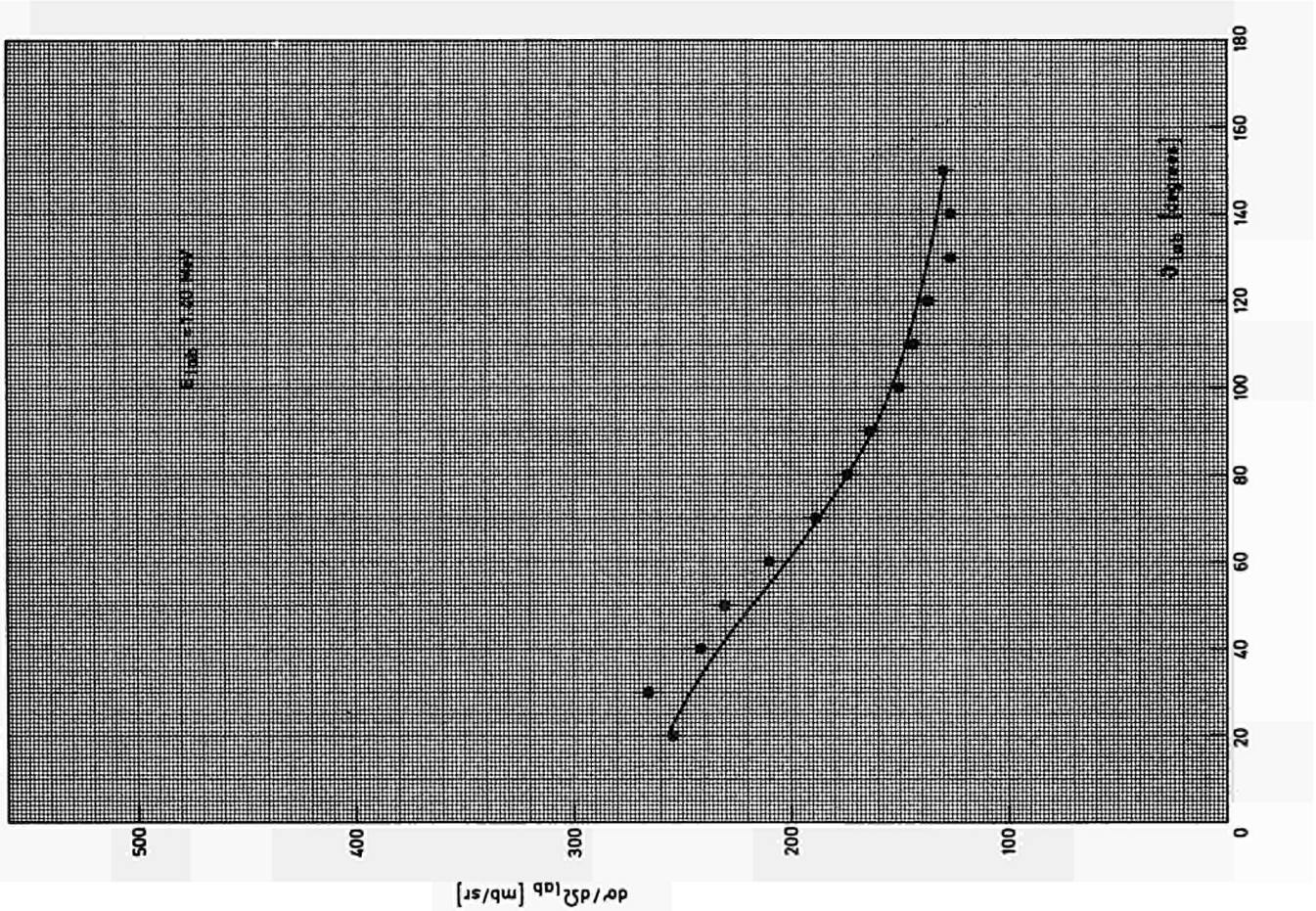
dσ/dΩ_lab [mb/sr]
0
100
200
300
400
500
0
20
40
60
80
100
120
140
160
180
θ_lab [degrees]

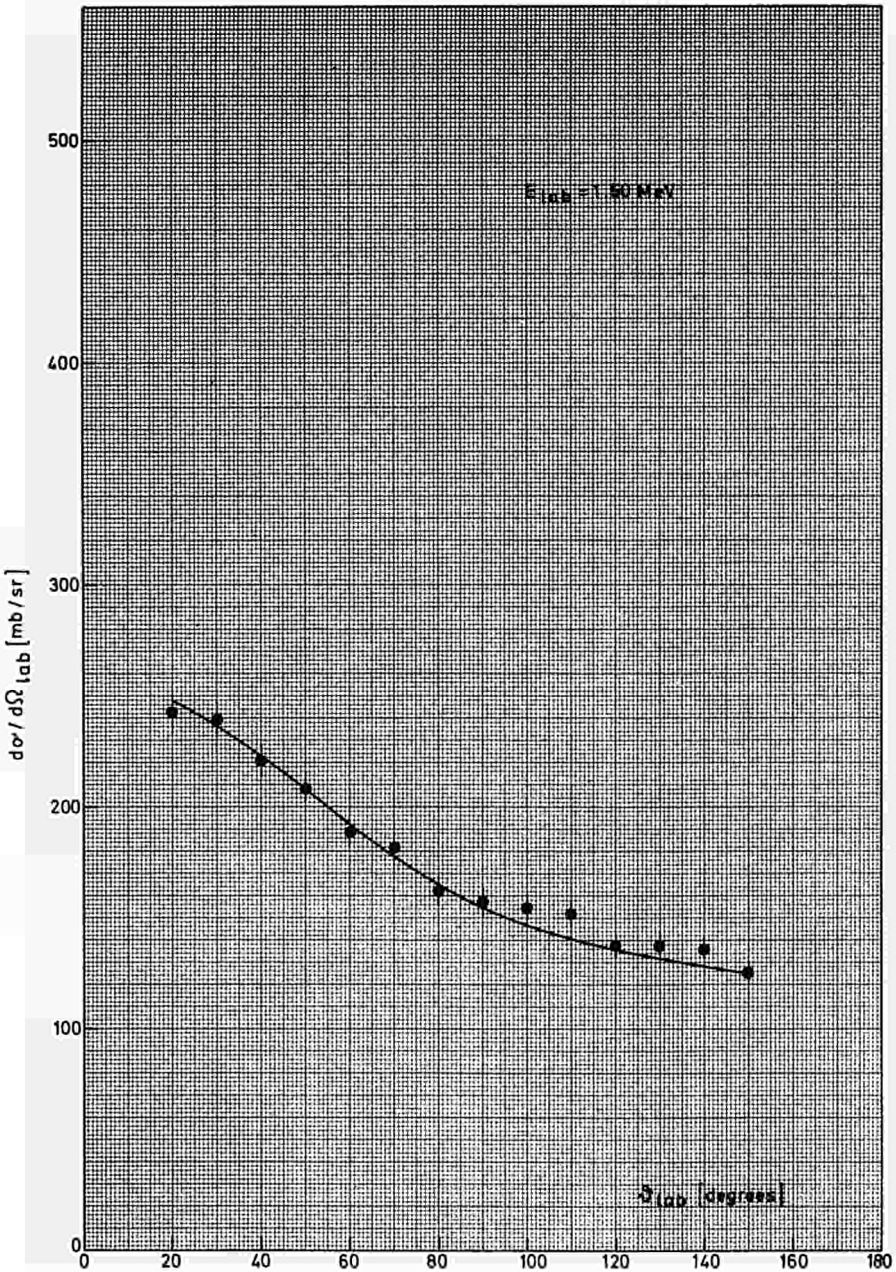
E_{lab} = 1.50 MeV
$d\sigma/d\Omega_{lab}$ [mb/sr]
ϑ_{lab} [degrees]
0
100
200
300
400
500
0
20
40
60
80
100
120
140
160
180

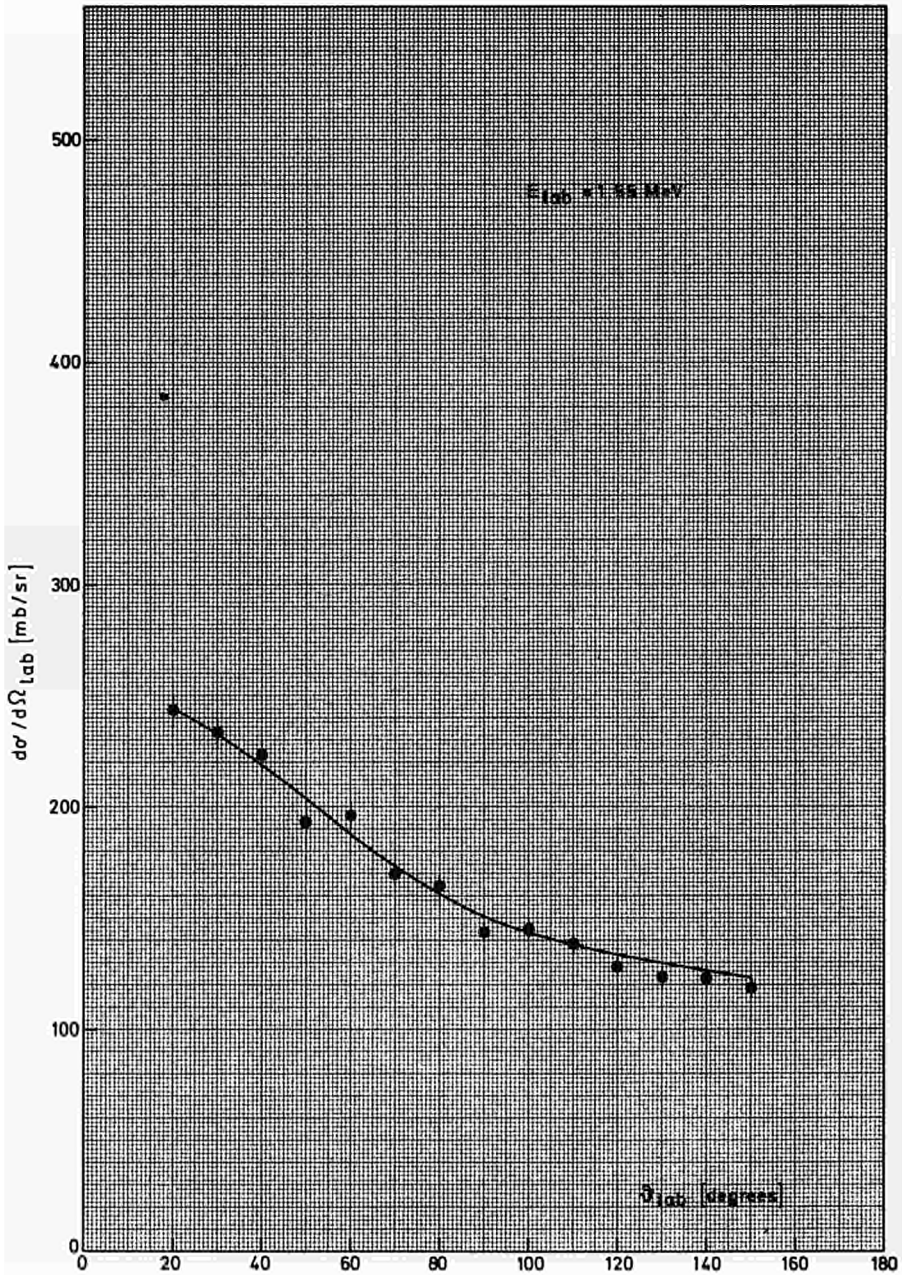
E_{lab} = 1.55 MeV
$d\sigma/d\Omega_{lab}$ [mb/sr]
ϑ_{lab} [degrees]
0
100
200
300
400
500
0
20
40
60
80
100
120
140
160
180

E_{lab} = 150 MeV
$d\sigma/d\Omega_{lab}$ [mb/sr]
ϑ_{lab} [degrees]
0
20
40
60
80
100
120
140
160
180
100
200
300
400
500

E_{lab} = 155 MeV
$d\sigma/d\Omega_{lab}$ [mb/sr]
ϑ_{lab} [degrees]
0
20
40
60
80
100
120
140
160
180
100
200
300
400
500

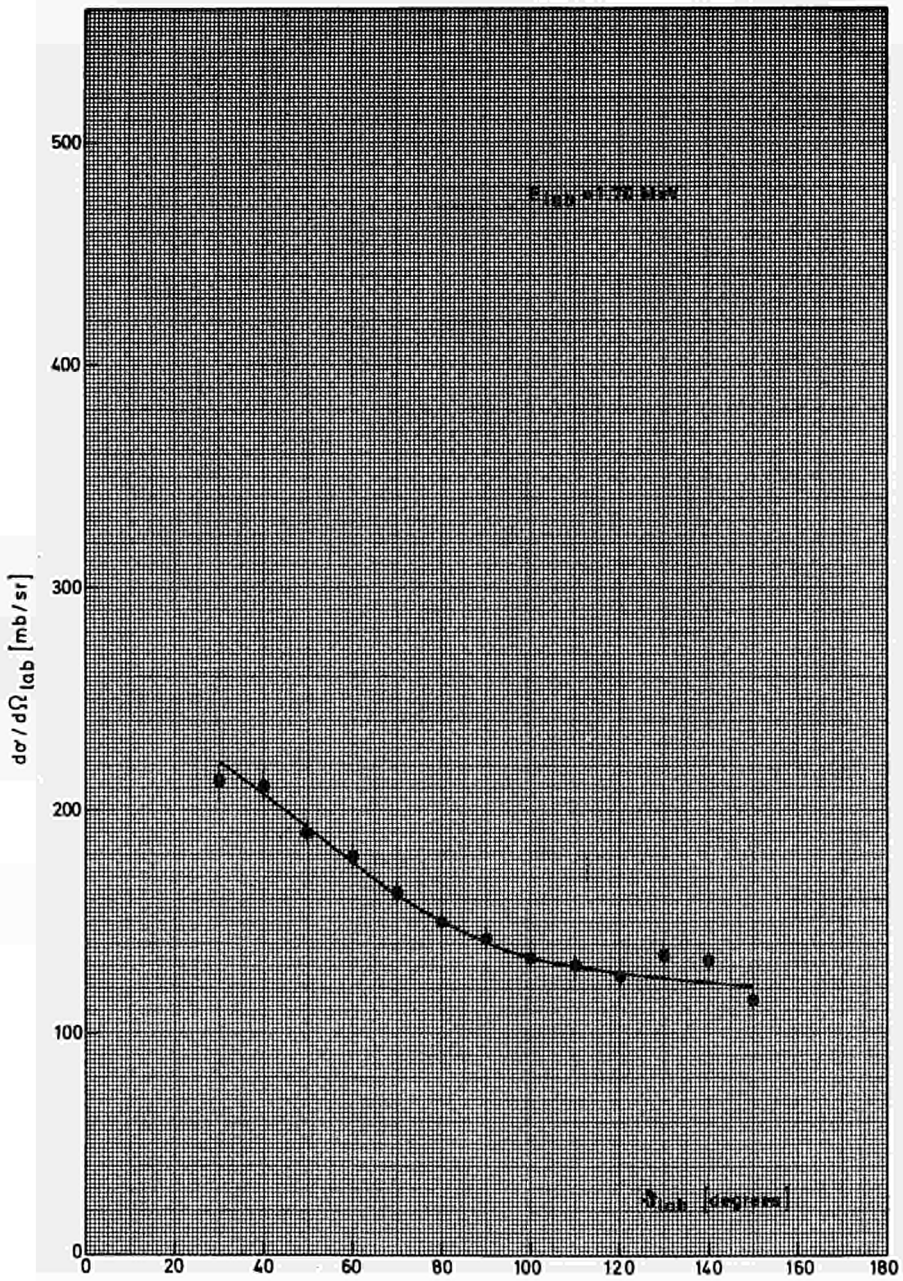
dσ / dΩ lab [mb/sr]
500
400
300
200
100
0
0
20
40
60
80
100
120
140
160
180

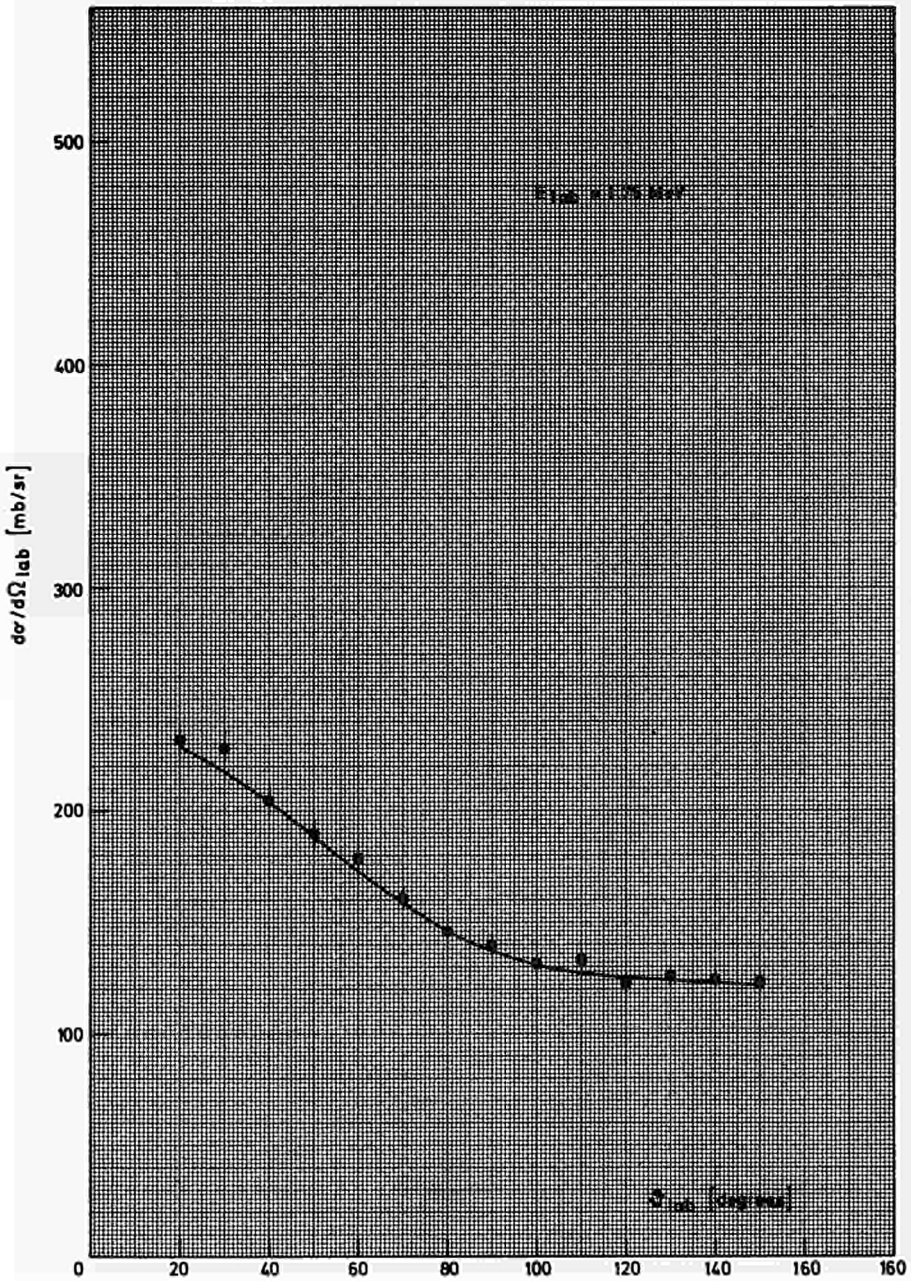
dσ/dΩ lab [mb/sr]
500
400
300
200
100
0
20
40
60
80
100
120
140
160

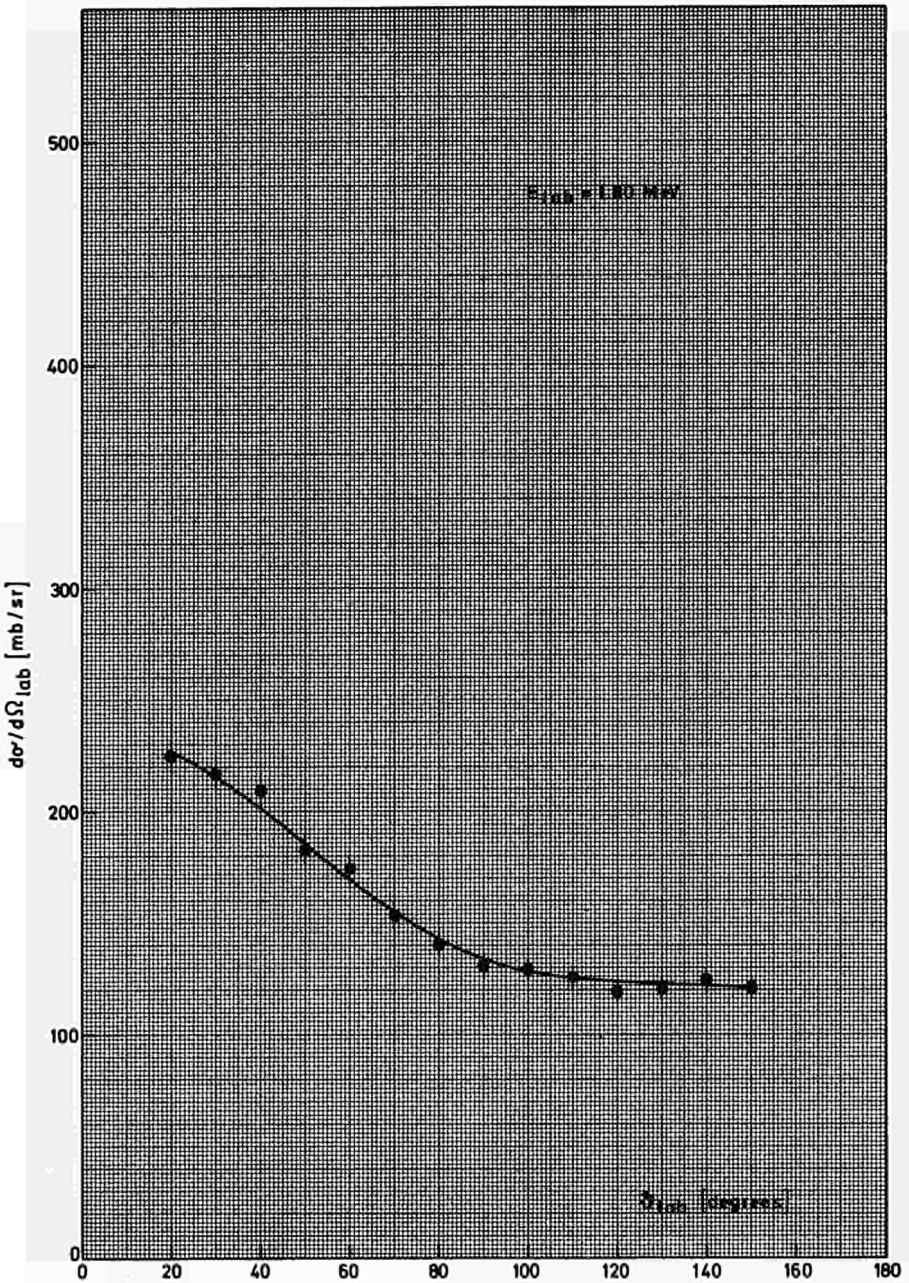
E_{lab} = 130 MeV
$d\sigma/d\Omega_{lab}$ [mb/sr]
ϑ_{lab} [degrees]
0
100
200
300
400
500
0
20
40
60
80
100
120
140
160
180

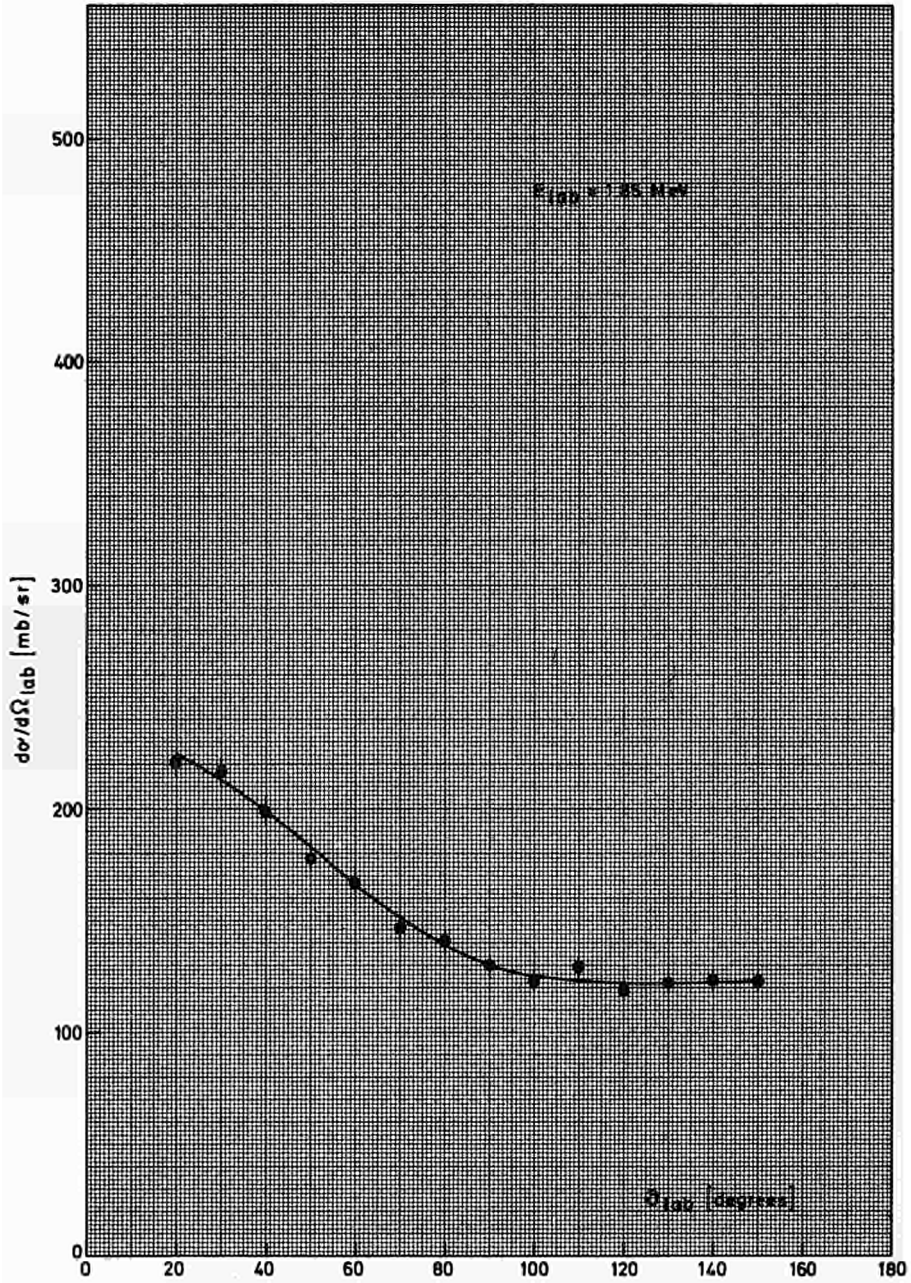
E_{lab} = 135 MeV
$d\sigma/d\Omega_{lab}$ [mb/sr]
ϑ_{lab} [degrees]
0
100
200
300
400
500
0
20
40
60
80
100
120
140
160
180

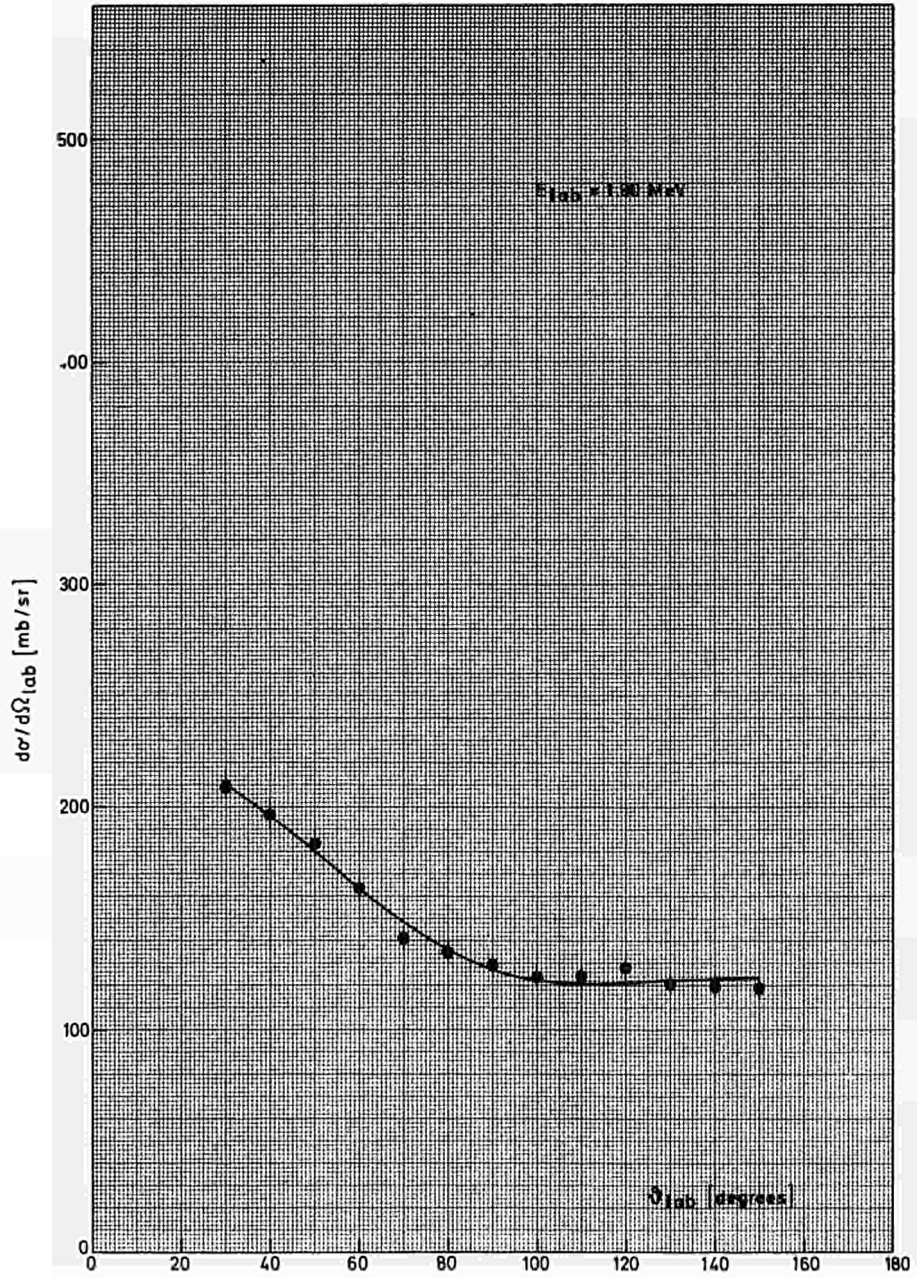
E_{lab} = 1.90 MeV
$d\sigma/d\Omega_{lab}$ [mb/sr]
ϑ_{lab} [degrees]
0
100
200
300
400
500
0
20
40
60
80
100
120
140
160
180

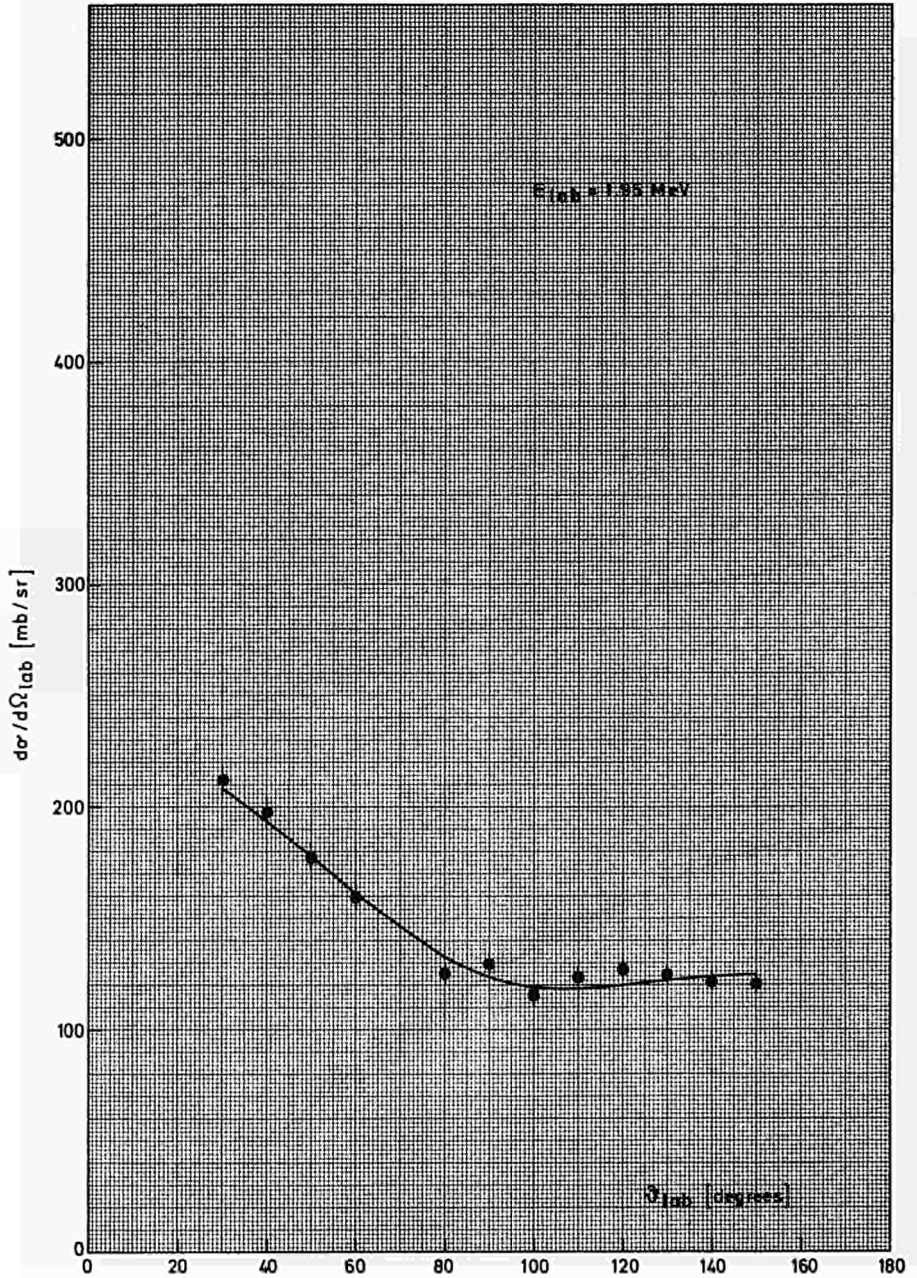
E_{lab} = 1.95 MeV
$d\sigma/d\Omega_{lab}$ [mb/sr]
ϑ_{lab} [degrees]
0
100
200
300
400
500
0
20
40
60
80
100
120
140
160
180

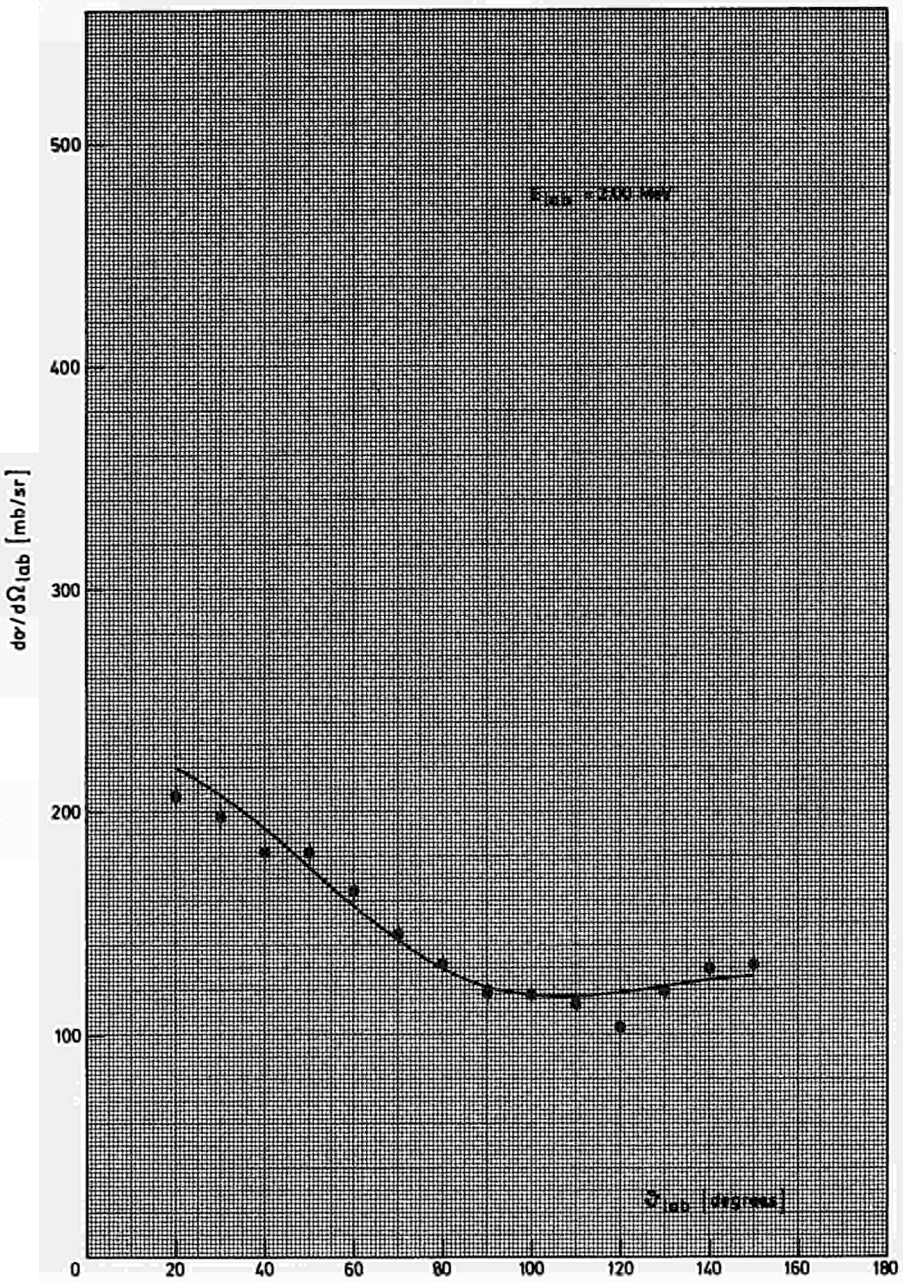
E_{lab} = 200 MeV
$d\sigma/d\Omega_{lab}$ [mb/sr]
ϑ_{lab} [degrees]
0
20
40
60
80
100
120
140
160
180
100
200
300
400
500

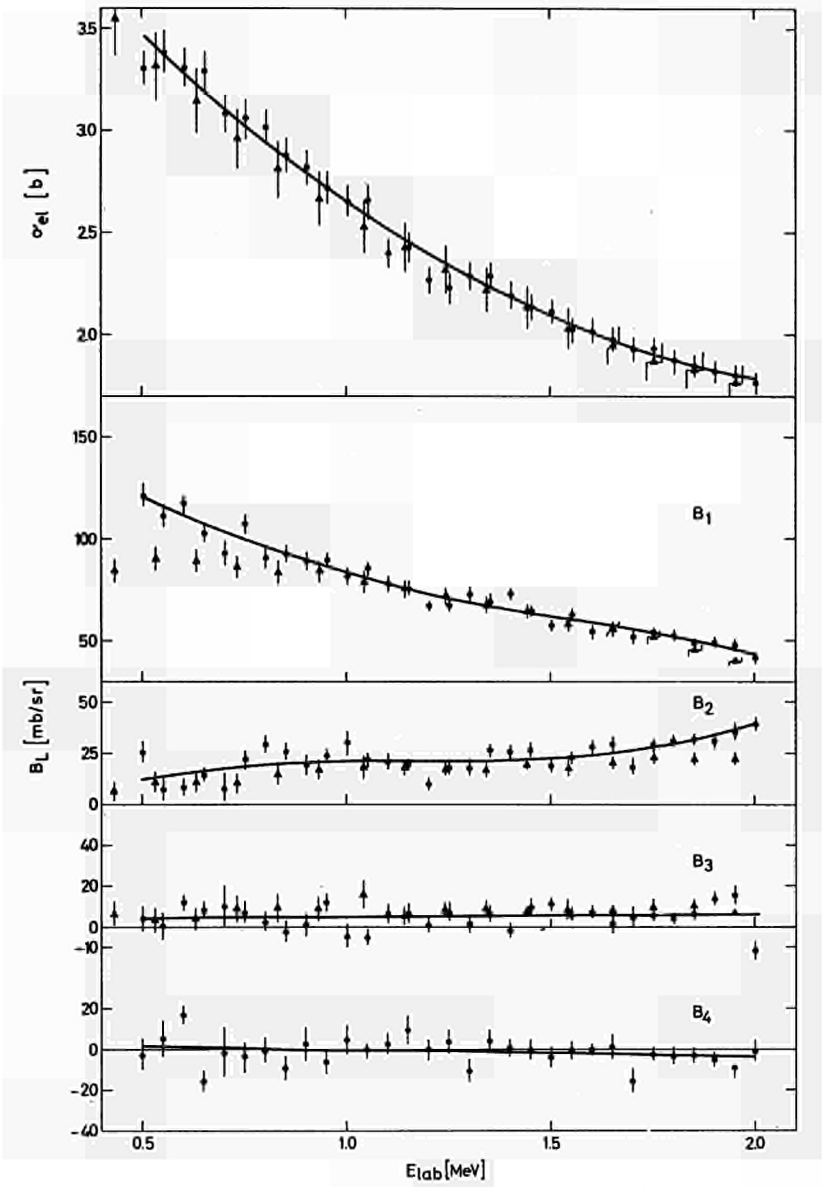
σ_{el} [b]
35
30
25
20
B_1
150
100
50
B_2
50
25
0
B_3
40
20
0
-10
B_4
20
0
-20
-40
B_L [mb/sr]
0.5
1.0
1.5
2.0
E_{lab}[MeV]

Fig.36

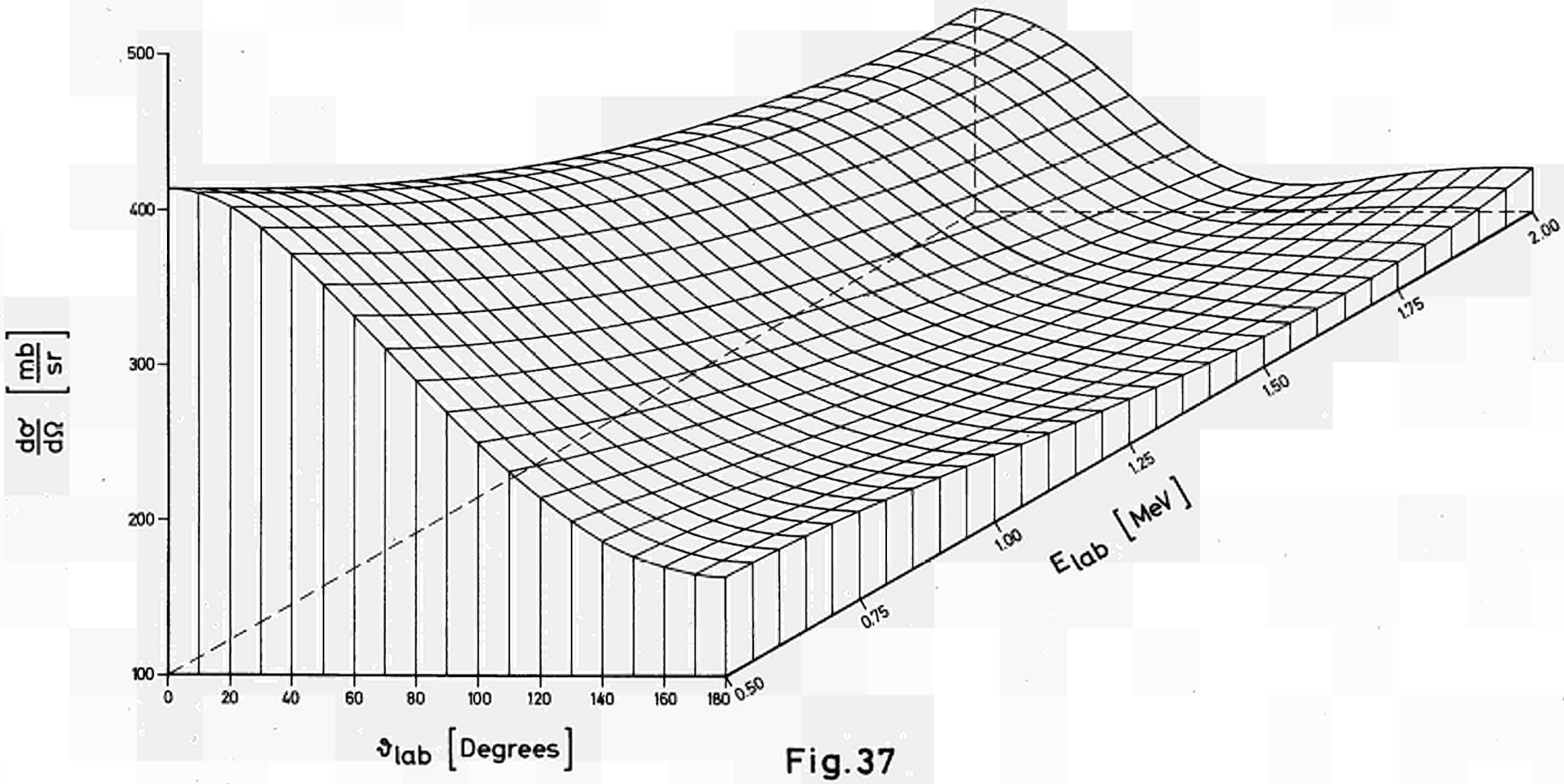
500
400
300
200
100
dσ/dΩ [mb/sr]
0
20
40
60
80
100
120
140
160
180
ϑlab [Degrees]
0.50
0.75
1.00
1.25
1.50
1.75
2.00
Elab [MeV]

Fig.37

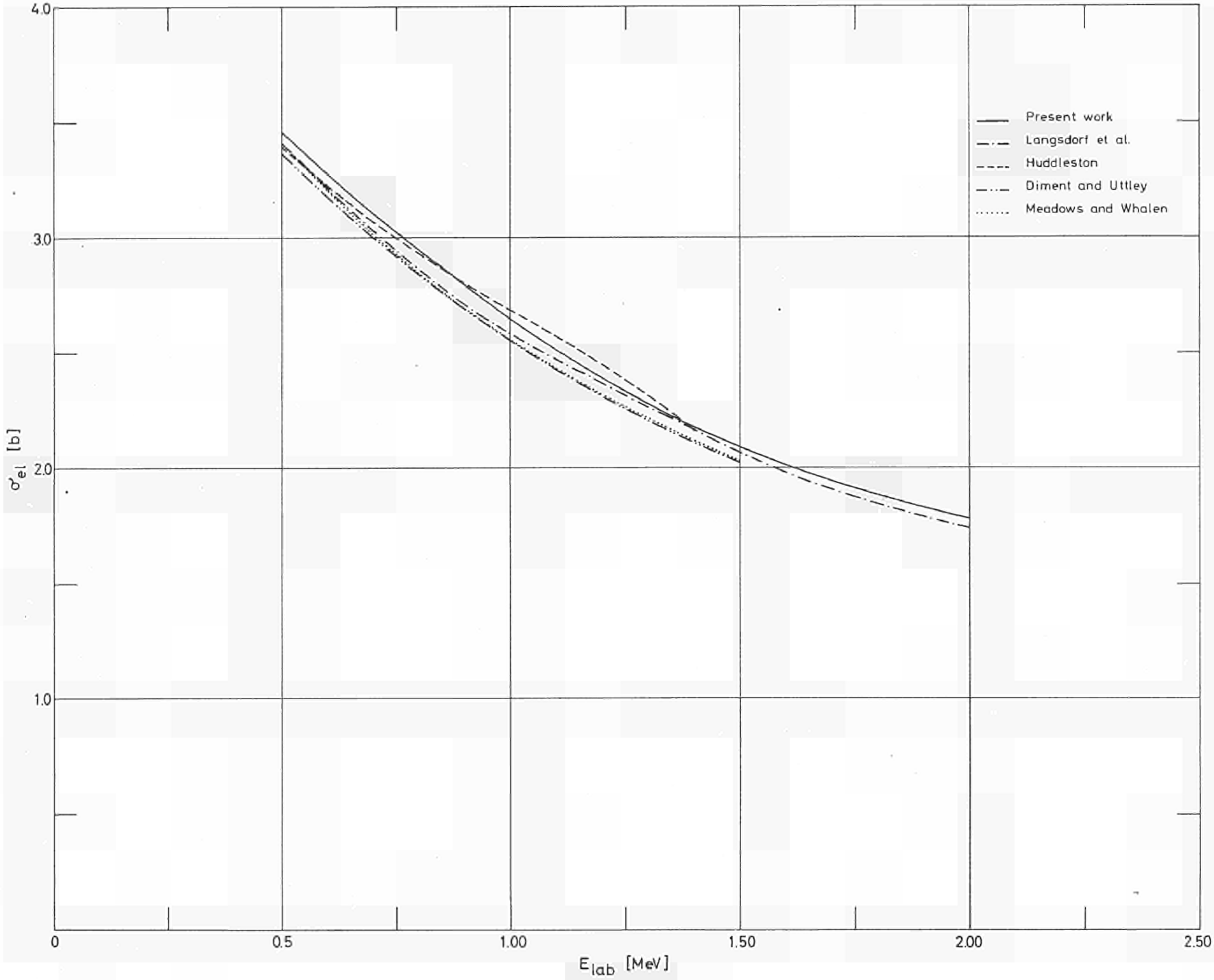
4.0
3.0
2.0
1.0
σ_{el} [b]
0
0.5
1.00
1.50
2.00
2.50
E_{lab} [MeV]
Present work
Langsdorf et al.
Huddleston
Diment and Uttley
Meadows and Whalen

Fig.38

NOTICE TO THE READER

All Euratom reports are announced, as and when they are issued, in the monthly periodical **"euro abstracts"**, edited by the Center for Information and Documentation (CID). For subscription (1 year : US $ 16.40, £ 6.17) or free specimen copies please write to :

Handelsblatt GmbH
"euro abstracts"
Postfach 1102
D-4 Düsseldorf (Germany)

or

Office de vente des publications officielles
des Communautés européennes
37, rue Glesener
Luxembourg

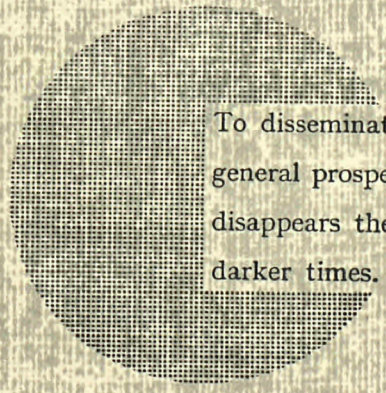

To disseminate knowledge is to disseminate prosperity — I mean general prosperity and not individual riches — and with prosperity disappears the greater part of the evil which is our heritage from darker times.

Alfred Nobel

SALES OFFICES

All reports published by the Commission of the European Communities are on sale at the offices listed below, at the prices given on the back of the front cover. When ordering, specify clearly the EUR number and the title of the report which are shown on the front cover.

SALES OFFICE FOR OFFICIAL PUBLICATIONS OF THE EUROPEAN COMMUNITIES
37, rue Glesener, Luxembourg (Compte chèque postal Nº 191-90)

BELGIQUE — BELGIË
MONITEUR BELGE
Rue de Louvain, 40-42 - 1000 Bruxelles
BELGISCH STAATSBLAD
Leuvenseweg 40-42 - 1000 Brussel

DEUTSCHLAND
BUNDESANZEIGER
Postfach - 5000 Köln 1

FRANCE
SERVICE DE VENTE EN FRANCE DES PUBLICATIONS DES COMMUNAUTES EUROPEENNES
26, rue Desaix - 75 Paris 15e

ITALIA
LIBRERIA DELLO STATO
Piazza G. Verdi, 10 - 00198 Roma

LUXEMBOURG
OFFICE DE VENTE DES PUBLICATIONS OFFICIELLES DES COMMUNAUTES EUROPEENNES
37, rue Glesener - Luxembourg

NEDERLAND
STAATSDRUKKERIJ
Christoffel Plantijnstraat - Den Haag

UNITED KINGDOM
H. M. STATIONERY OFFICE
P. O. Box 569 - London S.E.1

Commission of the European Communities
D.G. XIII - C.I.D.
29, rue Aldringer
Luxembourg